Chapter 3

The Proton Synchrotron (PS): At the Core of the CERN Accelerators

Donald Cundy and Simone Gilardoni

3.1 Introduction

The PS accelerator

After almost 60 years of honourable service, the history of the CERN Proton Synchrotron, PS, is marked by successes and discoveries, intimately linked to the CERN history. Today, the PS is the beating heart of the LHC (Large Hadron Collider) injector complex, the last of the countless successes of this incredible and versatile machine. At the origin of this longstanding success is the foresight of the CERN founding fathers who in the early 1950s took the risk to bet on a new technique in accelerator design called strong focusing [1]. Their "scientific and technological" audacity paved the road of CERN's future, but also encouraged others to embrace the same spirit of technological enterprise. Conceived as a prototype machine with a life time of only a few years the PS would not only exceed all expectations, but also inspire the design of all the modern circular machines. The PS was and still is an invaluable tool for beam physics studies, and was the cradle of high energy physics for many years, until more powerful machines like the ISR (Chapter 4) started in turn the era of the hadron colliders.

The PS is a synchrotron accelerating particles up to 28 GeV [2–5]. The energy was chosen based on physics considerations, i.e., study particle interactions at the GeV scale, but also economic ones. The initial energy was set well beyond the few GeV scale, up to 30 GeV, but the first machine design was considered too expensive and technologically risky. Fortunately for the future generations of physicists, CERN Council rejected the recommendation of W. Heisenberg to reduce the energy, thus the cost, to 20 GeV, and decided to keep the machine design that reached 25 GeV.

A synchrotron like the PS is a circular ring where particles during acceleration from the lowest to the highest energy are always kept on the same orbit with a constant radius of curvature [Box 2.1]. This is realized by increasing, synchronously with the energy change, the strength of the magnetic elements generating the force that counteracts the centrifugal force acting on the particles. Whereas the synchrotron concept was applied at other places before CERN, like the Cosmotron accelerator in the USA at BNL, the PS was unique with the first ever implementation of the concept of strong-focusing, i.e., the presence in the machine lattice of dedicated beam focusing elements, the quadrupoles. These are elements with properly shaped magnetic fields to control the physical size of the beam, thus limiting the maximum beam dimensions, much as in normal optics lenses would focus the light rays. This can be reached, as in classical light optics, by alternating focusing lenses with defocusing ones, from which the name of alternating gradient lattice was derived. The concept of strong focusing, also called alternating-gradient focusing, was invented in the early 1950s [1], and boldly adopted by CERN in 1952 for the future PS in an incredible gamble: while the cost of the construction could be significantly reduced, because the new focusing principle held the promise of smaller beam and therefore smaller beam elements, this novel idea had never been tested on a real accelerator. The PS was a resounding success, closely followed by its sister synchrotron in the USA, the AGS. All modern accelerators for high energy applications, including the LHC, are based on the strong focusing principle.

The implementation of this technique took a very particular form in the PS [2]: C-shape combined function magnets reaching 1.4 T at 28 GeV were chosen, which combine the functions of bending and focusing of the beam in the same magnetic element, a choice partially motivated by the heritage of the previous accelerators. However, the first-time use of a strong focusing lattice opened also a Pandora's box full of new issues in accelerator physics: having the beam circulating without being lost in the first few turns (the full accelerating cycle takes about 2.4 s, i.e. up to about 1 million turns) requires tight tolerances on magnet geometry and relative magnet alignment of the order of few 100 μm on a machine of 628 m circumference. The required magnetic field quality (i.e. precision) had never been achieved before. For example, the relative spread in deflecting strength of the magnets had to be less than 5×10^{-4}. Despite these challenges, measurements repeated in 2014 confirmed that the magnets, constructed in the first half of the 1950s, were actually better than specified, leaving a sense of awe and admiration for such work realized with the technology available at that time. Another example, the calculation of the beam stability to define the required tolerances, was realized using the first generation of computers available in the UK.

RF Acceleration **Box 3.1**

The particles in synchrotrons and colliders [Box 2.1] are accelerated by one or more RF cavities. These devices provide an accelerating electric field to increase particle energy per turn or manipulate the bunches (e.g. splitting, merging). Their simplest version is a pill-box in which an oscillating electromagnetic (e-m) field is generated; this provides the longitudinal electric field (Fig. 1). The field does not propagate into the adjacent vacuum chamber; to do so would require a much higher frequency e-m field.

For all cavity types, the e-m field oscillates with a frequency f_{rf} (wavelength $\lambda = c/f_{rf}$) which is a multiple h of the revolution frequency f_0 of the particle $f_{rf} = h \cdot f_0 = h \cdot c \cdot \beta / C$, where $\beta = v/c$ and C the circumference of the ring. Since the RF field is oscillating, the beam cannot be continuous and the particles must come in groups, called bunches. The harmonic number h defines the maximum number of bunches in the beam. The bunch to bunch distance is nC/h or in time n/f_{rf} with $n = 1, 2, \ldots$ Gaps in the beam can be generated by not filling the positions of a group of bunches, such as when required for injection or extraction. To enable transfer from one circular accelerator k to the next $k+1$, C_{k+1}/C_k must be the ratio of two positive integer numbers. For example, LHC/SPS = 27/7, SPS/PS = 11/1. Bunch to bunch distance is preserved at transfer.

If the particle speed is varying during acceleration, which is the case until the particle energy E exceeds by far its rest energy, E_0, f_{rf} has to vary in synchronism with f_0 and the resonance eigenfrequency f_{ef} of the cavity needs to be tuned as f_{ef} has to be very close to f_{rf}. The difference between f_{ef} and f_{rf} is determined by stability criteria [Highlight 3.3]. When β approaches 1, or the cavity is used exclusively at a particular energy, only residual tuning is required to make f_{ef} close to f_{rf} to maintain stability. A remotely controlled mechanical device, the tuner, performs this task changing the shape of the cavity slightly. Depending on cavity use, the shape is optimized taking into account RF power requirements, RF power dissipation, peak surface electric fields, and space constraints. This can lead to shapes quite different from the pill-box (Fig. 2). In case powerful acceleration is required, many cavities (cells) are combined in a structure in which either a travelling wave (e.g. 200 MHz RF structure in the SPS) or a standing wave is set up. The RF power is injected via a coupling loop at a point along the structure and is transmitted by em coupling between the cells.

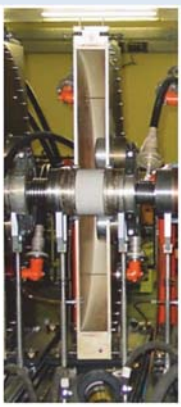

Fig. 1. (Left) Open PS 200 MHz 75 cm diameter (λ/2) pill-box cavity, with ceramic gap connected to the beam tube [5].

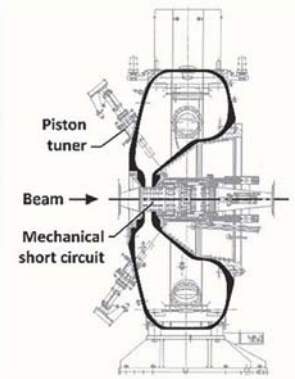

Fig.2. (Right) Cross-section of the PS 80 MHz, 1.8 m diameter cavity, shaped to house the short circuit [5].

The machine took its final shape under the direction of J. Adams during a construction period between 1956 and 1959. The ring is composed of a sequence of 100 main magnets interleaved by 100 straight sections hosting (i) the auxiliary magnets, (ii) the elements for injecting and, later, extracting the beams, (iii) the accelerating radio-frequency (RF) cavities [Box 3.1]. The combined-function magnets shown in Fig. 3.1 are also equipped with a series of windings on their pole-faces to make fine adjustments to the field, a feature substantially enlarging the versatility of the PS.

The machine was assembled on top of a floating floor, mechanically separated from the CERN ground to avoid external disturbances to the machine alignment, e.g. arising from a deformation of the foundation by rain or even earthquake, which would adversely influence the beam orbit.

The first beam was accelerated to 26 GeV in a memorable night of the 24 November 1959, opening both a new era in accelerator physics and in accelerator-based high energy particle physics, an event celebrated in due form on the following day (Fig. 3.2).

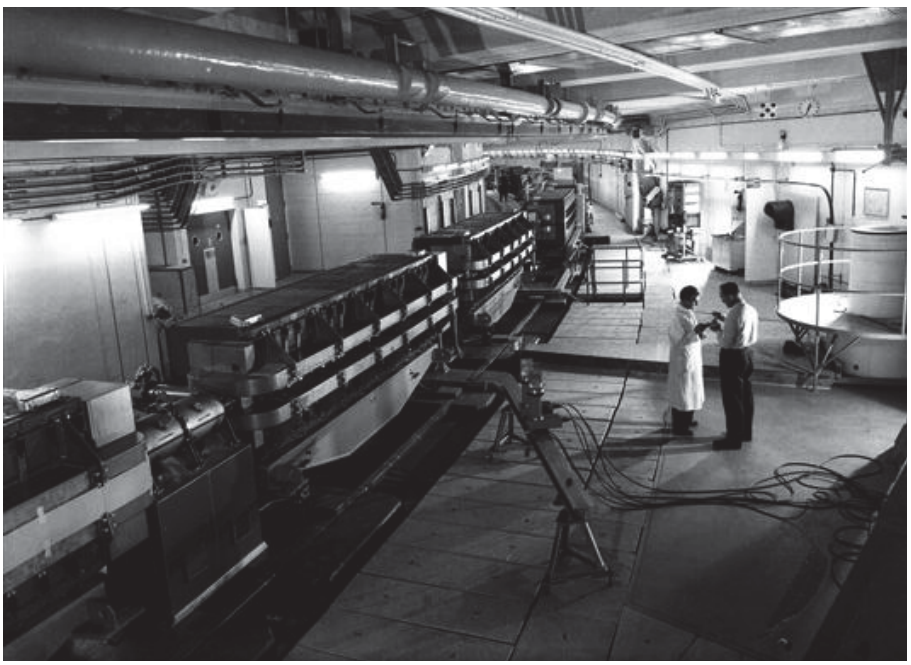

Fig. 3.1. View of the PS ring showing the combined-function magnets.

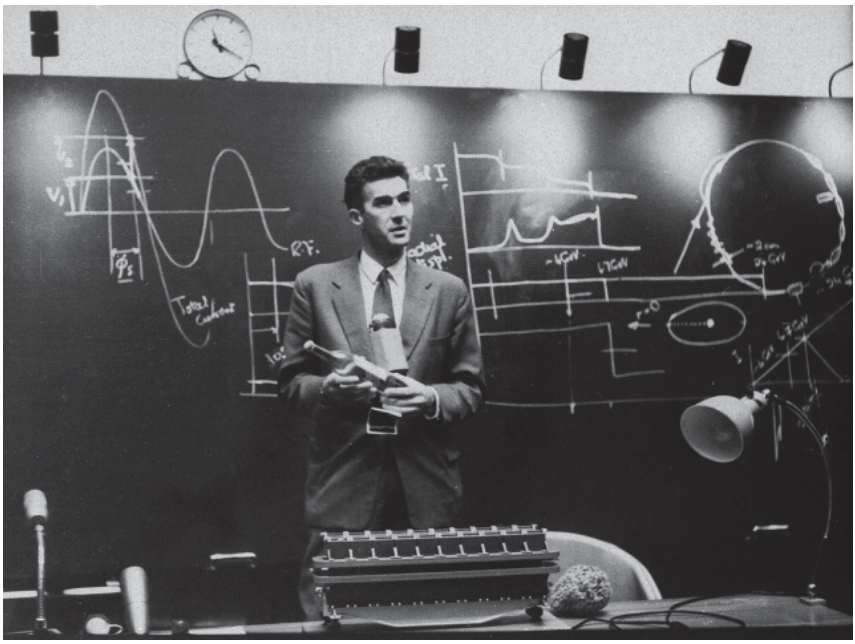

Fig. 3.2. J.B. Adams, the PS project leader, announcing acceleration to 24 GeV in the PS. The Vodka bottle in his hand was a gift from Dubna to be consumed on the occasion of the PS surpassing 10 GeV, the energy of the Dubna Synchro-Phasotron.

Once the basic features of the accelerator were understood, the PS and its injection systems underwent a long series of gradual improvements of performance, reliability and versatility leading to new applications. One indication is the gradual rise of the PS intensity over the years spanning from the design value of ~10^{10} protons per pulse to more than 3×10^{13} achieved for the latest neutrino experiment (Fig. 3.3).

High energy physics research at the PS started first with internal targets and later in 1960 with dedicated beam lines receiving protons by fast or slow extraction. These novel beam extraction techniques were developed with the aim to suppress the originally installed internal targets, source of substantial beam loss, producing a high radiation dose to the machine elements, in particular to the main magnets, and a serious risk to the machine lifetime. Extraction of the beam reduced the internal losses. The external targets allowed higher impacting intensities and could be placed at positions optimal for the experiments [Highlight 3.2].

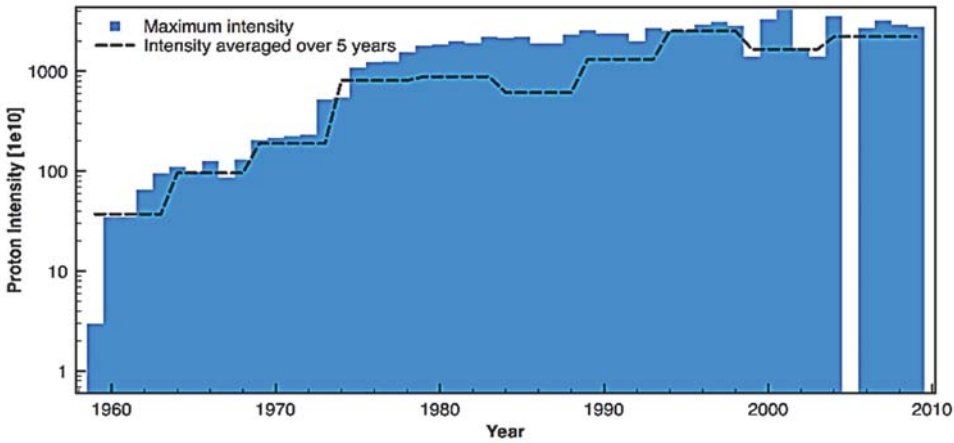

Fig. 3.3. Protons per pulse as a function of time. The PS was stopped for consolidation in 2005.

Special attention has always been paid to the PS injectors [6]. The first injector was a linear accelerator constructed by industry (Linac1) providing 50 MeV protons. In 1965 an improvement programme of the PS was launched together with the approval of the ISR (Chapter 4). The PS beam intensity was increased by inserting a small synchrotron between Linac1 and the PS, the PS Booster (PSB) [Highlight 3.4]. This novel type of accelerator of very compact design combines four synchrotrons in one ring with common bending and focusing magnets. Its potential turned out to be enormous, probably even a surprise to its designers, brought to life by a tenacious development since its first operation in 1972. Not only helped it to increase the intensity in the PS by combining the output of the four rings, but the 16 times higher beam energy compared to Linac1 made the beam stiffer moving the intensity limit at PS injection beyond the intensity provided by the PSB. This intensity limit was later further raised by successive steps in the PSB's output energy from the original kinetic energy of 0.8 GeV to 1.4 GeV. This was indispensable to catch up with the steadily increasing PSB output intensity, raised by a factor eight since 1972. However, the PS did not remain the only client of PSB: ISOLDE [Highlight 3.8] had been moved from the SC to the PSB in order to benefit from the higher proton intensities at the PSB, an elegant solution, because ISOLDE uses only those PSB pulses which are not injected into the PS. A new CERN-designed 50 MeV linac (Linac2) was added in 1978 to improve not only the performance but also the availability of the PSB. Linac1 had already earlier shown its versatility by accelerating deuterons and alpha particles for the ISR but when no longer needed for proton operation it was modified to provide oxygen and sulphur beams to the PS for fixed-target physics

at the SPS. However, it was unsuitable for the acceleration of heavier ions so one resolved to replace Linac1 with Linac3 of modern design providing nowadays mainly lead ions to the LHC, but also indium and argon ions for the SPS.

The venerable PS still provides a variety of hadron beams including antiprotons (Chapter 6). It also supplied electrons and positrons of 3.5 GeV to the SPS for LEP (see Chapters 5 and 7). To this end, it was equipped with the appropriate acceleration systems, injection/extraction elements and a 600 MeV electron-positron linac as injector feeding a small accumulation ring preceding injection into the PS. In view of improving the LHC injector performances, Linac2 will be replaced by a new linac accelerating negative hydrogen ions to 160 MeV (Linac 4). In order the cope with the concurrent intensity increase, the PSB output energy will be raised in another step to 2 GeV, 2.5 times the design energy, another proof of the PSB's amazing inherent potential.

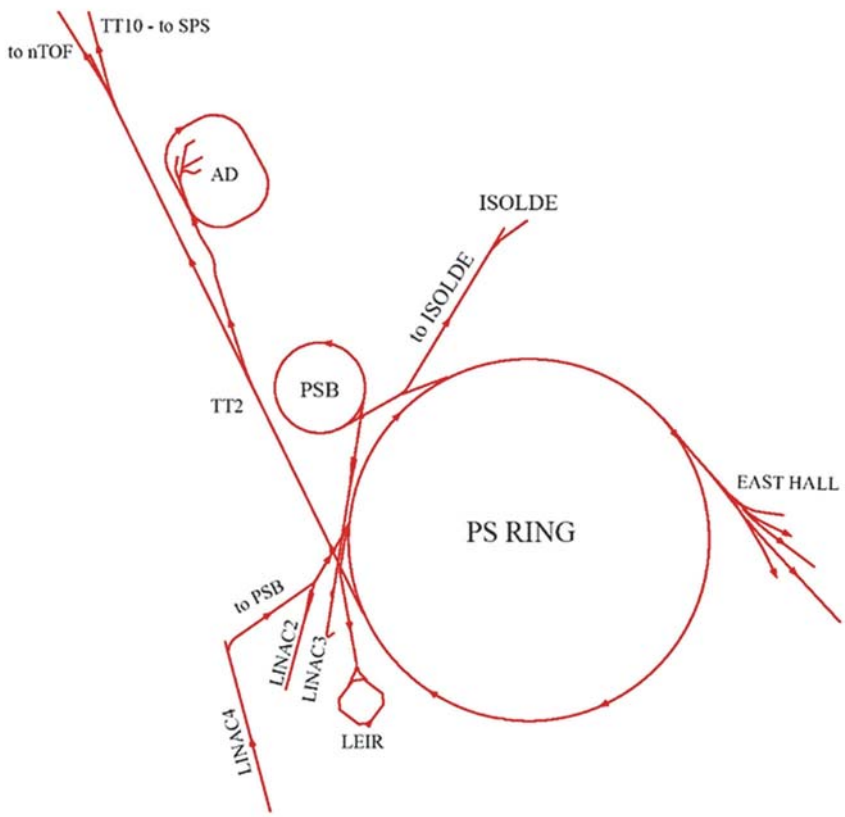

Fig. 3.4. Layout of the injectors and beam lines to the experiments.

The PS is still at the core of producing proton and ion beams as shown in Fig. 3.4 for fixed-target physics at the PS, the Antiproton Decelerator (AD), the SPS, and for the LHC. The LHC collider operates with two different bunch spacing, either 50 ns or 25 ns, the latter being the design configuration. Subtle manipulation of the beam by RF [Highlight 3.3] determines this bunch spacing in the PS and the downstream accelerators. Continuing a 60-year long tradition of attentive care, its infrastructure is maintained to keep up with the ever-increasing demand. A shining example is the novel solid-state main power converter with capacitive energy storage replacing the more than 30-years old rotating machine, which used a flywheel or energy storage to smooth the load to the mains [Highlight 3.5]. The new technology proved to be so successful that it inspired colleagues of the sister synchrotron AGS in the USA to consider also replacing their rotating machine.

A most flexible design, high-quality components and vigorous consolidation programmes for the accelerator and its infrastructure are the basis for the surprising durability of this synchrotron which proved, every time it was called upon a new task, its adaptability, versatility and reliability. This venerable machine stayed and will stay for many years at the heart of the CERN accelerator complex, a fine example of the continuous (re)use of CERN infrastructure.

The PS experimental programme

When the CERN PS was ready for physics in 1960, particle physics had entered a Golden Age of "particle discovery". Strange particles, collected painstakingly using cosmic rays, were now being produced copiously at the proton synchrotrons. The electron-neutrino ν_e had been detected. The antiproton and the antineutron had been discovered. Parity Violation (PV) in Weak Interactions (WI) was proven in 1956. However, theoretical guidance was still weak or absent: the quark hypothesis was made in 1964, followed by the electroweak theory in the late 1960s, the SM by the end of the sixties, and the theory of strong interactions (QCD) in 1973 [Boxes 4.2, 6.4]. The physics landscape and major PS results are reviewed in [7].

The bubble chamber (BC), invented in 1953, had become, with gradual improvements, the detector *par excellence* [Box 3.3 and Highlight 5.7]. The hydrogen BC, providing a proton target, lent itself to the detailed study of particle production, whilst the heavy liquid BCs proved very useful in the study of weak decays of the new particles. However, these BCs have a serious drawback: the repetition rate, i.e. their data taking rate is very low and they lack the capability of selecting specific events.

Particles interacting with matter **Box 3.2**

To be detected, a particle must transfer some of its energy to the detector material [Box 6.3]. The nature of the interaction — electromagnetic (e-m), strong, weak — depends on the particle charge and quantum numbers. A *charged particle* excites (*ionizes*) the medium through which it passes: this can produce a measurable signal, the basis for most detectors. Tracking detectors record *ionization* produced along the trajectory of charged particles [Highlight 4.8]. The ionization energy loss dE/dx depends on the particle velocity v and may provide a measure of v; if the particle momentum p is known, its mass can be determined [Box 5.2]. Some media exhibit the property of *scintillation*: a charged particle traversing matter leaves a trail of excited molecules which release part of this energy as photons. Although only a few percent of the total energy loss, it is sufficient to detect a particle. Besides colliding with atomic electrons, a particle, shaken by the e-m fields in the material, emits *radiation* at a rate roughly proportional to E/m^2. This process is characterized by the *radiation length* X_0 of the medium, over which an $e^{\pm}$ has lost all but $1/e$ of its energy, and a γ-photon has a 2/3 probability to convert into a $e^{\pm}$ pair. Typical values of X_0 are 1.8 cm (Fe) and 300 m (air 1 atm). Above a critical energy E_C, radiation effects (bremsstrahlung for $e^{\pm}$, pair conversion for γ's) dominate over ionization energy loss. For $e^{\pm}$, E_C is a few tens of MeV for most materials; heavier muons have a critical energy of several hundred GeV. Two metres of iron absorb most particles except muons, so muons are usually measured behind hadron calorimeters [Highlight 7.10]. *Neutral particles* are not sensitive to e-m effects**.** If unstable, they can be detected by tracking charged decay products [Highlight 8.6]; if stable or long-lived (e.g. neutrons), detection is ensured via strong interactions in devices such as calorimeters [Highlight 4.10]. *Hadrons* — baryons (e.g. the proton) and mesons (e.g. the pion) — interact strongly, producing a *hadron shower*, a process characterized by the *nuclear interaction length* λ (for iron, $\lambda = 17$ cm), the mean path length over which energetic hadrons have a ~2/3 probability to interact inelastically. About 10 λ absorbs a 100 GeV hadron. Among *leptons,* neutrinos (ν), neutral, stable and weakly interacting, are the most difficult to detect: a 10 GeV ν has only a 10^{-7} probability to interact when crossing the Earth! To observe ν interactions requires massive detectors and large ν flux. A ν escaping from an interaction can be inferred from its "*missing momentum*" vector by measuring all detectable particles. In e-m collisions a charged particle is deflected stochastically: the *mean deviation angle* is proportional to $\sqrt{t}/p$, where t is the thickness of the material in units of X_0. This impacts on the accuracy of tracking and explains the need for detectors with low total t. Other e-m energy loss mechanisms are (i) the *Cherenkov effect*: a charged particle traversing matter produces a trail of polarized molecules along its path, which depolarize and emit radiation. If the velocity $v > c/n$, n being the refractive index of the medium, there is a direction along which the radiation adds coherently, giving "Cherenkov light" (analogous to a sonic boom), emitted at the *Cherenkov angle* θ_C, where $\cos\theta_C = c/nv$ [Highlights 7.8, 8.10]; and (ii) *Transition Radiation (TR)*, which occurs when a charged particle passes between media of different permittivity. It is used to identify ultra-relativistic electrons [Highlight 4.9].

This motivated the development of "electronic", triggerable detectors, such as spark chambers, scintillation counters and threshold Cherenkov detectors for particle identification [Boxes 3.2 and 6.3]. It culminated in the invention of the "Multi-wire proportional chamber (MWPC) in 1968 [Highlight 4.8]. Counter and emulsion experiments studied secondary particle production (π, K, antiprotons) from various targets located in the PS beam. These studies were to have strong impact on the design of separated beams that were soon to be built.

While the PS machine was built in a remarkably short time, CERN's start of its physics programme was rather more shaky. There were, it should be noted, not so many physicists participating in the research programme at CERN at that time, as the larger member states were still pursuing their national projects. Fortunately for the development of particle physics, there was still at that time strong political and financial support given to both nuclear and particle physics.

In 1960 one of the big puzzles in particle physics was the muon, which decays into an electron and two neutrinos. What prevents the muon from decaying into an electron and a gamma ray? An elegant hypothesis gives the electron and muon a hidden property ("quantum number"), which stipulates the existence of two neutrinos *species*, one related only to the muon, ν_μ, and another one associated to the electron, ν_e. Neutrino scattering it was argued, could test this hypothesis: $\nu_\mu + n \rightarrow p + \mu^-$ and $\nu_e + n \rightarrow p + e^-$.

A source of ν_μ is the pion, decaying essentially into a muon and a neutrino. Early in 1960 it had been argued that pions, produced at accelerators like the PS, would give enough ν_μ's to perform a conclusive experiment. CERN jumped on this idea with great enthusiasm, because of its conceptual simplicity and physics importance. In the South Hall pions were produced on an internal target in the PS, which subsequently decayed in a 20 m space, followed by some 20 m of iron and concrete shielding. The main detectors were the CERN and the Ecole Polytechnique BP3 heavy liquid bubble chambers containing a total of about a ton of CF_3Br Freon. The expected rate was around one event per day. However, a last minute beam survey showed that the pion flux would be an order of magnitude below design and the experiment was stopped. CERN lost its chance for a big discovery, the muon neutrino. Only one year later, in 1961, the two-neutrino hypothesis was confirmed in a Brookhaven experiment using the same method and a spark chamber detector!

Despite this sobering setback, neutrino physics would develop into a very important field of research at CERN and elsewhere. The radioactive decay of particles due to the weak interaction occurs at relatively low energies. In contrast, neutrino scattering would probe the weak interactions at much higher energies and

Imaging detectors **Box 3.3**

These provide an image of particle tracks, usually recorded photographically.

Nuclear emulsion (NE) is a photographic plate with a thick layer of emulsion of uniform grain size. Compact and dense, it has the best spatial resolution of all, at the μm level. A crossing charged particle sensitizes the grains. After development, tracks are visible and measured with a microscope. NEs have undergone a renaissance, coupled to fast precise electronic detectors, which point to the region of interest.

The *cloud chamber (CC)* is a sealed environment containing a supersaturated vapour of water or alcohol. Charged particles ionize the vapour and the ions act as nuclei for condensation. Mist forms around the ions to produce a visible track. In a *pulsed CC or Wilson chamber* (C.T.R. Wilson, Nobel 1927), a diaphragm expands the volume which cools and initiates condensation. Positrons and muons were discovered in cosmic rays using CCs. A *diffusion CC* is continuously sensitive, but needs cooling.

The *bubble chamber* (*BC*, A. Glaser, Nobel 1960), is similar in principle to a CC: a cylinder is filled with a liquid heated to just below its boiling point. A piston suddenly expands its volume, lowering the pressure and driving the liquid into a superheated metastable phase. Microscopic bubbles form along the ionization track. Their size grows as the BC expands, getting large enough to be photographed. Adding a magnetic field gives the momentum. More than 100 BCs were built [1], from very small to very large. The largest contained up to 40 m^3 of liquid hydrogen or heavier liquid (e.g. freon) and were used to record millions of images. Momentum resolution depends on the BC size, the magnetic field and the bubble size, ranging from typically 200 μm to 700 μm in diameter in BEBC [Highlight 5.7]. To study charm requires bubbles of 30 μm. Photographing such details limits the depth of field of the camera and the observable volume. This led to develop small rapid cycling BCs, e.g. LEBC [1].

The BCs were facilities, operated by large laboratories and used by many groups, leading to international collaborations, sharing the scanning and measuring of BC photos. Ever more elaborate analysis methods were developed, implying semi-automatic data recording and the use of powerful computers. These pictures, providing an intuitive view of physics events, helped to popularize the field. But restricted to fixed target physics, unable to be triggered and of low pulse rate, BCs could not give access to rare events and were progressively abandoned.

The *spark chamber* (*SC*) [2] uses the breakdown induced by a strong electric field locally around the particle trajectory. These "sparks" can be photographed or recorded electronically. A sequence of SCs provide a BC-like detailed view of the particle track. The two-neutrino US experiment (Chapter 3.1) used the first large SC set up. The largest one at CERN was the Omega spectrometer [Highlight 3.7]. *Streamer chambers* with shorter high-voltage pulses and image enhancement also used gaseous breakdown providing bubble-chamber type views of particle collisions.

From 0.01 Hz for CC, the pulse rate went to 0.3 Hz in BEBC and up to 20 Hz in SC. Discoveries made with these devices were essential in establishing the SM [Box 6.4].

[1] G.G. Harigel *et al*., (ed.), Proc. Conf. on Bubble Chambers, *Nucl. Phys. B, Suppl.* **36** (1994).
[2] R.P. Schutt, (ed.), *Bubble and Spark Chambers* (Academic Press, New York 1967).

would also allow to investigate the interior of the nucleon. Neutrino scattering would shed light on the fundamental nature of this mysterious weak interaction. At high energies, it was understood, a new mechanism has to be invoked, a particle, technically called "Intermediate boson" (IB), had to exist to transmit or "mediate" this interaction. This idea was worked out in the 1960s, although its mass was a mystery, justifying early searches at quite low masses. The chase for the IB would become one of the grand successes of CERN (Chapter 6).

There were other questions: is the "lepton property", the so-called lepton number conserved? Could a neutrino interact with a nucleon without changing into a charged lepton, i.e. besides the known "Charged Currents" (CC) of muon and beta decay, did "Neutral Currents" (NC) exist?

Towards neutral currents

CERN had learned its lesson: To run a viable neutrino research programme neutrino beams of adequate intensity were required. Step 1 was to maximize the pion flux, achieved by extracting the PS proton beam towards an external target in the direction of the experiments. Step 2 was a real breakthrough: the ingenious invention by S. van der Meer (Nobel Prize 1984) of a pulsed magnetic horn, focusing the pions, produced with different momenta and angles at the target, towards the detector and hence maximizing the neutrino flux [Highlight 3.6].

The beam was ready in 1963; the detectors were the CERN Heavy Liquid BC (HLBC) and a 15 ton spark chamber (SC) setup. The BC team would study the neutrino reactions in detail and measure cross-sections of specific processes. The SC group was primarily searching for the possible production of the IB (W^+ or W^-) with a mass below 2 GeV in the strong electric field of a heavy nucleus:

$\nu_\mu + \text{Nucleus} \rightarrow \mu^- + \text{Nucleus} + W^+$, with $W^+ \rightarrow \mu^+ + \nu_\mu$ or $W^+ \rightarrow e^+ + \nu_e$.

At the September 1963 Siena Conference, the two experimental teams presented their preliminary results, the BC with a couple of hundred events and the SC setup with many thousands. The former presented results on the cross-section measurements of the elastic process $\nu_\mu + n \rightarrow \mu^- + p$, the quasi-elastic process $\nu_\mu + p \rightarrow \mu^- + \Delta^{++} \rightarrow \mu^- + p + \pi^+$, on the energy dependence of the total cross-section and many other topics. The latter reported several di-muon candidates but could not say if they were W decays. The future was decided in a local trattoria: a very large heavy liquid BC with its splendid detail about the interactions was the way to move forward. It had to have a large target mass for a reasonable interaction rate and several interactions in length to distinguish pions from muons.

The proposal made to the French CEA was accepted and funded in 1964. In 1965 CERN agreed to host the heavy-liquid BC and to build a new neutrino beam. The BC was a cylinder 4.8 m long and 1.9 m in diameter with a volume of 12 m^3,

bright field illumination, six cameras and a magnetic field of 2 T. It would be known as Gargamelle (Fig. 3.5, left). The intellectual father and project leader was A. Lagarrigue (Fig. 3.5, right).

While waiting for Gargamelle, the CERN HLBC, which had been doubled in size, was filled with propane and exposed to the new beam. About this time a US group studying neutrino electron scattering at a nuclear reactor had reported a single electron signal three orders of magnitude greater than theoretically expected. A careful search for single electrons in the HLBC propane photos did not find any event, placing new upper limits on the "neutral current" processes $\nu_\mu + p \rightarrow \nu_\mu + p$ and $\nu_\mu + p \rightarrow \nu_\mu + n + \pi^+$. The reported claim was eventually withdrawn.

When data taking started in 1971 with Gargamelle, priority was given to measure the CC total cross-section and to probe the nucleon structure. The reason was that electron scattering experiments at SLAC had shown the nucleon to contain point-like constituents. Combining neutrino data with the electron data would allow to measure the charge and net number of these point-like particles.

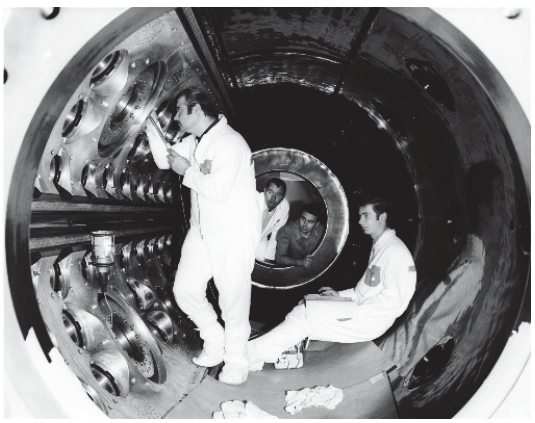

Fig. 3.5. Left: inside Gargamelle. Right: A. Lagarrigue, the driving spirit of Gargamelle.

However, early 1972, priorities were reversed. The Electroweak (EW) theory, unifying the weak and electromagnetic interactions, had been completed [8]. Crucially, it predicted the existence of a heavy *neutral* Intermediate Boson. Neutral Current (NC) events would therefore occur, revealed by a single recoil electron or by hadron production as in a CC event, but without a muon (Fig. 3.6). All efforts were devoted to scanning Gargamelle photos for single electrons and searching NC candidates with hadronic energy greater than 1 GeV. Studies on possible background events convinced the collaboration that neutrons coming from neutrino interactions in material around the detector were the only significant

background, which however could be evaluated and controlled. In addition, one NC candidate event with a single electron had been found in the antineutrino exposure where this background was negligible.

A competing US experiment produced contradictory results and some confusion. However, sure about their results, the Gargamelle collaboration announced and published their evidence for the existence of neutral currents in July 1973 with the measured ratio NC/CC = 0.21 ± 0.03 for neutrinos and NC/CC = 0.45 ± 0.09 for antineutrinos [9]. This result was a turning point in the history of particle physics, leaving little doubt about the validity of the EW SM, allowing to predict the weak bosons masses with small errors and opening the modern era of precision tests of the SM. The premature death of A. Lagarrigue probably deprived the neutral current discovery of a Nobel Prize.

Other results followed. The total neutrino-nucleon cross-section was found to rise linearly with energy, consistent with point like objects in the nucleon, confirming with the weak probe the earlier SLAC observation with the electromagnetic probe. Combining both results showed that these constituents have indeed fractional charges.

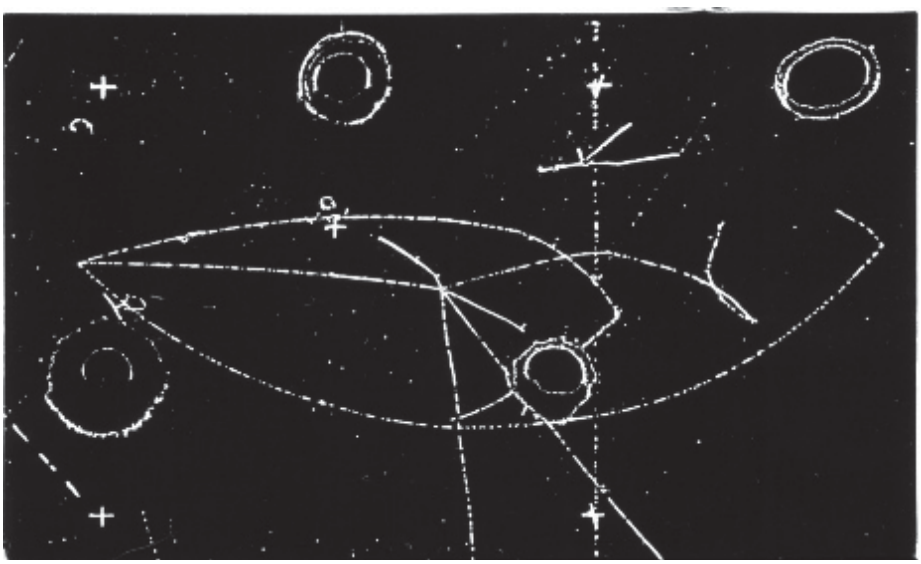

Fig. 3.6. A neutral current event in Gargamelle. The neutrino beam enters from the left. All three tracks from the collision vertex either undergo very large angle scattering or interaction, proving that no muon is produced.

Interestingly, a neutrino beam was again derived from the PS in the early 1980s, aiming at the West Area neutrino detectors in search of neutrino "oscillations", i.e. their "morphing" along their way, from a muon-neutrino to an electron- or tau-neutrino. As realized later, neutrino oscillations indeed exist, but with periodicities not experimentally accessible at CERN. Nevertheless, the experiments, e.g. PS191, were visionary and pioneering in their concept.

After its difficult start the PS neutrino programme had turned out to be quite remarkable!

Other programmes

In 1960 CERN reorganized their experimental activities in response to the changing nature of the experiments and their techniques. With the aim of strengthening the research programme the experiments using counter techniques and those with bubbles chambers were supported in separate dedicated Divisions.

Hydrogen bubble chambers at the PS

During the PS time BCs increased in size from 30 cm to 2 m size, and were exposed to an increasing variety of hadron beams.

Coping with the enormous number of BC photos led to R&D programmes for the machine inspection (scanning) of the BC pictures. Semi-automated or fully automated measurement equipment on digitizing tables were developed; computer programs were developed to analyse and interpret the events [10].

The list of new particles and resonances became ever longer. Cross-sections were measured with great precision and particle production mechanisms studied in detail. The CERN PS experiments made significant contributions. Various theoretical models came and went until it was eventually realized that this zoo of particles could be best described by the model of fractionally charged quarks by M. Gell-Mann and G. Zweig, then a visitor in the CERN Theory Division [11].

One of the most important spinoffs of the BC program was sociological: it attracted many European university teams in particle physics and contributed to fostering a culture of fruitful collaboration among different nationalities: The building of this aspect of the "CERN model" got on its way.

Experimentation with electronic detectors

Research, increasingly concentrating on phenomena occurring with very small cross sections and using a variety of particle beams, motivated a rapid growth and diversification of the electronic detectors. Scintillation counters, Cherenkov detectors and spark chamber became the "workhorses" of ever more sophisticated experiments based on these electronic techniques. The 1968 invention of the Multiwire Proportional Chamber (MWPC) by G. Charpak, Nobel Prize 1992, truly initiated this electronic revolution.

Initially, the spark chambers events were recorded photographically, soon to be replaced by acoustic, magnetic core and magnetostrictive readout. In 1964 a meeting was held at CERN on "Film-less Spark Chamber Techniques and Associated Computer Use" [12]. This led to the wire spark chamber, invented at CERN, in which the plates were replaced by wires. The "sparks" produced electrical pulses in the wires, which were directly logged into a computer. This was the start of using computers for monitoring and data recording of the experiments.

One experiment, using a combination of dipole and quadrupole magnets and an electrostatic separator, followed by a very sophisticated Time-of-Flight system discovered the production of anti-deuterons in proton–beryllium collisions, preceding a similar observation at BNL by a few weeks. The existence of the bound state of antinucleons was essential for the proof of the existence of antimatter, as Dirac liked to emphasize. It also lent credence to the concept of a fundamental symmetry, the so-called Charge–Parity–Time Reversal (CPT) symmetry [Box 2.2], fundamental to quantum field theories, such as the SM.

The rise of electronic detectors motivated a bold decision to develop an "electronic bubble chamber", a large 1.8 T magnetic field volume, instrumented with spark chambers, capable of selecting (triggering on) specific reactions. The device was known as OMEGA [Highlight 3.7]. At the PS it was used from 1971–76 to study meson spectrometry and rare modes of hadronic reactions, and subsequently in a productive program at the SPS, with spark chambers being replaced by MWPCs.

CP violation [Box 3.4] was discovered at Brookhaven in 1964 and the result quickly confirmed at CERN, eliminating some theoretical models and correcting some erroneous claims made elsewhere.

Experiments using the interference between the charged two-pion decay of K_S and K_L performed precise measurements of the K_S–K_L mass difference, the CP violation amplitude and phase [Highlights 5.5 and 5.6]. In 1969 one of these experiments began to use the first very large MWPC chambers. In 1972 a setup using wire chambers and a lead glass array proved that the ratio of the CP violating amplitudes of the two-pion charged and neutral decay of K_L was equal to unity to a 6% level. It would take another 20 years to know that they differ from unity at the per mille level (Chapter 5, SPS).

Kaon mixing and CP violation **Box 3.4**

The K^0 shows a puzzling behaviour: It decays via the weak interaction in ~10^{-10} s into two $\pi^{\pm}$ or two π^0, called K_1, and 600 times slower into three pions (π^+, π^-, π^0 or 3 π^0), called K_2! The explanation is that the K^0 can change into an anti-K^0 ($\overline{K}^0$), and vice versa, by virtual decay and recombination. The decay modes observed are the symmetric (K_2) and antisymmetric (K_1) quantum state combinations of K^0 and $\overline{K}^0$. This seems complicated, but is simple and has a classical analogue of two coupled pendula, Fig. 1.

For two identical pendula, coupled by a spring (Fig. 1), only two modes of oscillation can exist: parallel (P) and antiparallel (AP). One can ascribe a *symmetry* to the pendula under which the AP (P) mode is considered an even (odd) state. The spring is at work in the AP mode only, and hence it will have a slightly higher frequency than the P mode. If the spring is not perfect, it costs energy and the AP mode will decay away quicker than the P mode. Setting in motion e.g. the right pendulum (left of Fig. 2) the spring will transfer energy between the two pendula, such that the left one starts and the right one comes to rest, and vice versa. This is due to the interference (beating) between the two modes. The antiparallel mode is damped and will decay away first.

In our particle picture, assume the *motion* of the left (right) pendulum to represent a K^0 ($\overline{K}^0$), Fig. 2. The right pendulum describes an initial *pure* $\overline{K}^0$ state. The spring provides the interaction which changes the K^0 and $\overline{K}^0$ into each other. Fig. 2, right part, shows that the K^0-$\overline{K}^0$ system can be considered as the superposition of the P (odd) mode, representing a K_2, and the AP (even) mode, representing a K_1. The spring is not perfect and the antiparallel mode K_1 is damped first, leaving the long lived K_2. The two different K_1 and K_2 decay rates are reproduced. The decays were considered to be invariant under CP, i.e. CP to be a good or conserved symmetry in the weak interactions [Box 2.2]. The symmetry ascribed above to the pendula is the mechanical equivalent to CP symmetry seen in the kaon system.

If CP were a perfect symmetry, then the CP odd K_2 should not decay into a CP even 2π state: but in 1964 one found that it did at the 10^{-3} level, showing that CP is violated in K^0 mixing: K^0 and $\overline{K}^0$ do not change into each other at the same rate. This kind of CP violation is demonstrated with the coupled pendula by connecting the spring at different positions on the K^0 and $\overline{K}^0$ arms. Then the energy transfer between the two pendula is not equal: the long-lived mode contains a small part of K_1, is no longer a pure CP state, and is called K_L. The short-lived mode contains some K_2 and is called K_S.

Due to mixing the amount of CP violation seen in the decay mode into two $\pi^{\pm}$ should be the same as for the decay into two π^0. This is only true down to the 10^{-6} level, where so-called *Direct CP violation* is also observed [Highlight 5.5]. Related effects are observed in the decay of B-mesons, particles containing a beauty quark [Highlight 8.6].

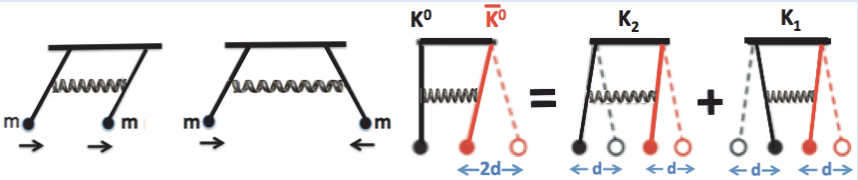

Fig. 1 Fig. 2

The PS measurement of the anomalous magnetic moment of the muon, $g - 2$, [Highlight 2.4], successfully continued the tradition started at the SC. With a 5 m diameter storage ring experiment (1967–1970) an accuracy of 3 parts in 10^4 was reached, to be superseded with a new storage ring of 7 m (1972–76), which reached an accuracy of 1 part in 10^5. Today, higher order QED calculations, including weak and hadronic corrections, predict $g - 2$ with an accuracy of 1 part in 10^6 and ongoing experiments elsewhere are being pushed to achieve an even higher accuracy. An observed slight discrepancy between the theoretical and experimental value, if it persists, would be a "smoking gun" for new physics.

Other facilities

Besides supplying protons for the SPS and the LHC, the PS also feeds some other very important facilities, ISOLDE, n_TOF and CLOUD.

The PS Booster's high intensity 1.4 GeV proton beam is directed onto special thick targets of the ISOLDE facility [Highlight 3.8], from which beams of radioactive isotopes are obtained.

For the n_TOF facility 20 GeV/c proton pulses, 6 ns long, are directed onto a lead target producing spallation neutrons in a wide energy range [Highlight 3.9]. These neutrons travel ~ 20 or 200 m to the experimental areas depending on the flux required. The energy of the neutrons is measured by time-of-flight. Research ranges from stellar nuclear synthesis to studies of nuclear reactor fuel cycles.

An experiment involving atmospheric, cosmic ray and particle physicists, and chemists, the Cosmics Leaving Outdoor Droplets (CLOUD) project, is studying the very complex processes of cloud formation under the influence of cosmic rays. The PS supplies the particle beams that simulate cosmic ray flux [Highlight 10.7].

3.2 Extraction: Getting the Beam to Leave the Accelerator

Massimo Giovannozzi and Charles Steinbach

Originally, the PS had used only internal targets. However, high radiation damage, due to absorption of secondary particles in the accelerator components, and low efficiency motivated the development of beam extraction and external targets. Fast extraction provides a beam with a length of one turn or less in one shot for users requiring high intensity in a short pulse, e.g. for experiments with bubble chambers; slow extraction skims off the circulating beam over many turns and is the choice for counter experiments preferring a long spill length and low instantaneous intensity to match their limited time resolution [13]. In 1963, the PS was the first synchrotron with a fast extraction system in operation and equipped with a successfully tested slow extraction system, initiating a leading position of CERN in the development and improvement of these key techniques.

Fast extraction

Fast extraction has been used for experiments in the East, West and South-East experimental areas of the PS and for sending beam to downstream accelerators (ISR, SPS, AA, LEAR, AD).

The principle is that a device producing a short (in time) deflecting magnetic field, called fast kicker, imparts an oscillation to the circulating bunches to be ejected so that they enter a deflecting magnet guiding them into the downstream transfer channel. This magnet is placed just outside the central aperture reserved for the circulating beam. One of its conductors acts as septum that separates the deflecting field from this aperture in order not to perturb the circulating beam. For clean extraction of a limited number of beam bunches, kicker rise and fall times had to be less than 80 ns, well below the 105 ns separation between two circulating bunches. During its first 60 years, the PS has known two different generations of kickers. The first, installed in the early 1960s, was of limited aperture and was retracted during injection when the beam size was large, and it was hydraulically positioned after beam acceleration. A stationary full aperture kicker system was proposed in 1964. It took nine years and two successive designs to obtain a satisfactory system with 12 separate modules. The magnets use ferrite for the yoke in the machine vacuum and form a 15 Ω delay-line. Figure 3.7 shows a schematic cross-section of such a kicker magnet (left) and one module (right).

The pulse forming networks (PFN) providing the driving pulse to the kicker are made of very low attenuation 15 Ω SF_6 pressurized polythene tape cables, charged to 80 kV in less than 4 ms by a resonant power supply. The discharge of the PFNs into the kicker is controlled by hydrogen thyratrons. The full-aperture kicker system was commissioned in 1974 and is still in use with high availability [14].

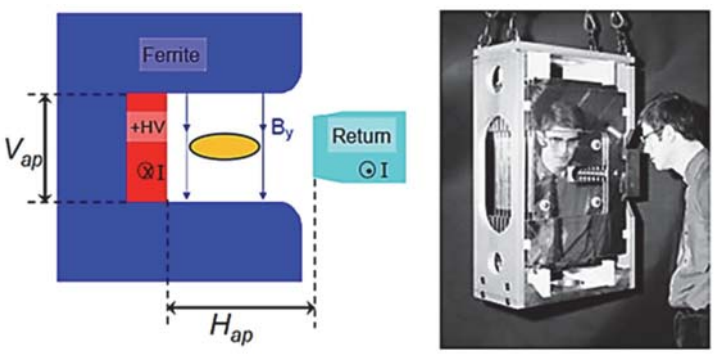

Fig. 3.7. Left: Schematic cross-section of the full-aperture kicker magnet showing the ferrite yoke, the one-turn coil (red/blue) and the beam to be deflected (yellow oval); Right: A module of this kicker with the gap for the beam seen in the middle of the shining front face.

Slow extraction

Slow extraction was introduced to provide primary beams to external targets for counter experiments. In this way external secondary beams can be produced with higher intensity and better quality than those from internal targets. During this extraction the focusing of the PS is adjusted such that the transverse oscillations of the particles grow due to a resonance driven by on-purpose installed magnetic lenses, which slowly increases the amplitudes of these oscillations until all particles have entered the deflecting field at the septum.

The first tests were conducted in 1963, reaching after improvements an extraction efficiency of 90%. In 1972 it became necessary to supply beams also to the new West hall. A new scheme was proposed based on a resonance occuring when the number of horizontal particle oscillation per turn, Q, is nudged to become a multiple of 1/3 (third-integer resonance). The resonance was driven by a standard quadrupole and a special semi-quadrupole combining quadrupolar and sextupolar fields. The scheme offered simultaneous beam sharing at will between internal targets and two external targets. The extraction efficiency reached 93% limited by the losses at the septa. The most recent scheme for proton slow-extraction was introduced in 1992 when the West hall extraction was suppressed. Taking into account that the internal targets had been eliminated by 1981 and the PS had to accelerate electrons and positrons for LEP, interleaved with proton cycles, its design used fewer and more standard magnetic elements for ease of maintenance, improved the ring vacuum, and provided component shielding against radiation from positrons or electrons. The first deflecting element of the extraction channel is equipped with a thin septum formed by an only 0.1 mm thick molybdenum foil to minimize beam loss (Fig. 3.8, left). It provides a deflecting electrostatic field of

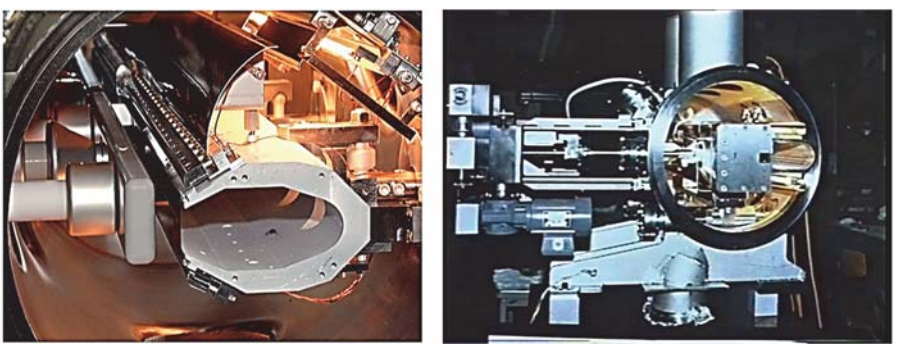

Fig. 3.8. Left: The electro-static deflector with a 0.1 mm septum in its vacuum tank; Right: Magnetic deflector with a 4 mm septum. The dark slot in the plate is the extraction channel while the aperture for the circulating beam is on the right of this slot.

10 MV/m (160 kV across a 17 mm gap) and is placed towards the inside of the ring to avoid exposure to radiation during lepton cycles [15, 16]. Further downstream, the deflected beam receives a second kick by a special magnet equipped with a thin (4 mm) septum before entering the transfer channel. This magnet also shares the ring vacuum and can be positioned remotely (Fig. 3.8, right). The extraction takes place at a particle momentum of 24 GeV/c providing 2×10^{11} protons per pulse over 400 ms (2×10^5 turns !) at the external target with an efficiency of 95%.

Multi-Turn Extraction

The development of this extraction method, called Continuous Transfer (CT), was driven by the need to fill the CERN SPS as uniformly as possible for fixed-target physics. Since the SPS circumference is eleven times that of the PS, the SPS could be filled by extracting the beam over several turns from the PS. The choice has been to fill the SPS with beam of two consecutive PS cycles, which terminate each time in an extraction over five turns at a particle momentum of 14 GeV/c. A gap of one 11^{th} of the SPS circumference is left without beam to accommodate the fall-time of the pulsed SPS injection elements. The principle is based on a careful choice of the number of horizontal particle oscillations, on a variable-strength closed orbit bump, and on an electro-static deflector with a thin (0.1 mm) septum that peels the beam off each cycle turning it into a spill of five PS circumferences in length.

In the quest for an improved extraction mode to substantially reduce the unavoidable beam loss on the first septum, a novel approach was proposed, named Multi-Turn Extraction (MTE). In this process the beam is split in a beam four turns long (“long beam”) and a central beam one turn long. This is achieved by generating, prior to extraction, stable islands in transverse phase space inside the circulating beam by crossing a resonance produced by appropriate non-linear magnetic fields. In this process the particles get trapped inside these islands thus generating around the central beam a new, well-separated stable beam which extends over four turns and closes in itself. By a controlled drift through the resonance these islands move towards larger transverse amplitudes until the horizontal separation between two beams exceeds the thickness of the septum. The resulting configuration in transverse phase space is a central beam around which the long beam closed in itself is wound. An example of the evolution of the beam distribution in horizontal phase space at a given azimuth along the circumference is shown in Fig. 3.9. Note that it is the same beam that appears in the four islands around the central beam.

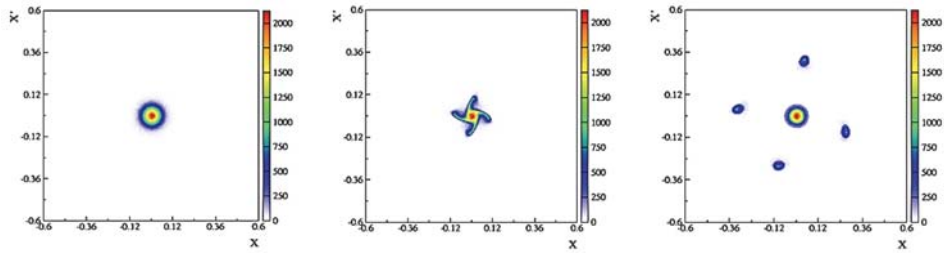

Fig. 3.9. Evolution of the horizontal beam distribution during resonance crossing in phase space (the ordinate is the horizontal momentum of the particles, while the abscissa is the horizontal position of the particles): The initial state (left); at resonance crossing particles are trapped inside the moving islands (centre); at the end of the process, the particles trapped in the islands are at larger amplitudes required for extraction (right).

Subsequently, a fast closed orbit bump created by two kickers, with a rise time short compared to the revolution time, is created with such an amplitude at the septum that the long beam enters the deflecting field region and is extracted over four turns while the central beam is not deflected. Finally, the central beam is extracted by a strong fast transverse kick creating a horizontal oscillation of sufficient amplitude making it enter the deflecting device. The timing is such that the central beam is contiguous to the long beam already transferred to the SPS.

The novelty of this method is that it replaces the brute force peeling by an intercepting device with a splitting performed by the non-linear resonance. This approach is superior as particle losses are limited to the fraction of the beam improperly deflected during the rise time of the fast orbit bump.

The proposed scheme was designed in 2006 and the first beam commissioning started in 2008. While the main concept of the beam splitting was quickly confirmed, the stability of the overall process has posed some problems. Moreover, the fraction of beam lost on the septum magnets during the rise time of the fast bump induced strong activation for which mitigation measures had to be devised [17]. This implied a major re-design of all fast extraction schemes, which were successfully commissioned by the end of 2014. This unique scheme has the welcome potential to reduce significantly the radiation dose to the equipment around the septum and, thereby, substantially increase component lifetime. As of September 2015 MTE has replaced CT as the operational extraction system from PS for SPS fixed-target physics. Thus, the PS moves closer to the ideal of loss-less extraction — the subject of a long-standing effort since its inception.

3.3 Acceleration and Bunch Gymnastics

Heiko Damerau and Steven Hancock

The basic function of the radio-frequency (RF) system is the acceleration of the particles grouped in bunches in synchronism with the rising magnet field which keeps them on orbit [Boxes 2.1 and 3.1]. In addition it is used to regroup the particles in user-defined bunch configurations along the orbit, different from the bunch sequence at injection, during the acceleration cycle, and to shape the final bunches before extraction according to the user requirement. Acceleration and bunch manipulations have to be performed avoiding beam instabilities and minimizing beam loss [18].

Key components of the RF systems are the cavities producing the accelerating electric RF field, the RF power supplies, ancillary equipment such as cavity tuners, devices damping undesired RF modes in the cavities, and control circuits to achieve the proper RF amplitude and phase. Two typical cavities are described.

The first example is the main RF system of the PS comprising 11 ferrite-loaded cavities each capable of delivering a peak voltage of 20 kV [19]. Originally it had been designed to operate on the 20^{th} harmonic of the revolution frequency for proton acceleration from 50 MeV (kinetic) injection energy to 28 GeV. Since the protons had only 30% of the speed of light at injection but nearly the speed of light at top energy, the RF had to cover a swing from 3 to 9.5 MHz. Today protons from the PS Booster (PSB) are injected at 1.4 GeV to limit adverse space charge effects on today's high-intensity beams, reducing the relative frequency swing during acceleration to only 10%. Nevertheless, presently a range from 2.8 MHz to 10 MHz is employed together with the possibility to independently use the cavities in groups, allowing beams of protons and ions to be accelerated and manipulated using harmonics in the range from 6 to 24. Figure 3.10 shows schematically a cavity consisting of two resonators with separate accelerating gaps and the ferrites used for tuning surrounding the vacuum tube. The tuning is accomplished by modifying the effective inductance of the ferrites through changing their magnetisation with the help of the current loops.

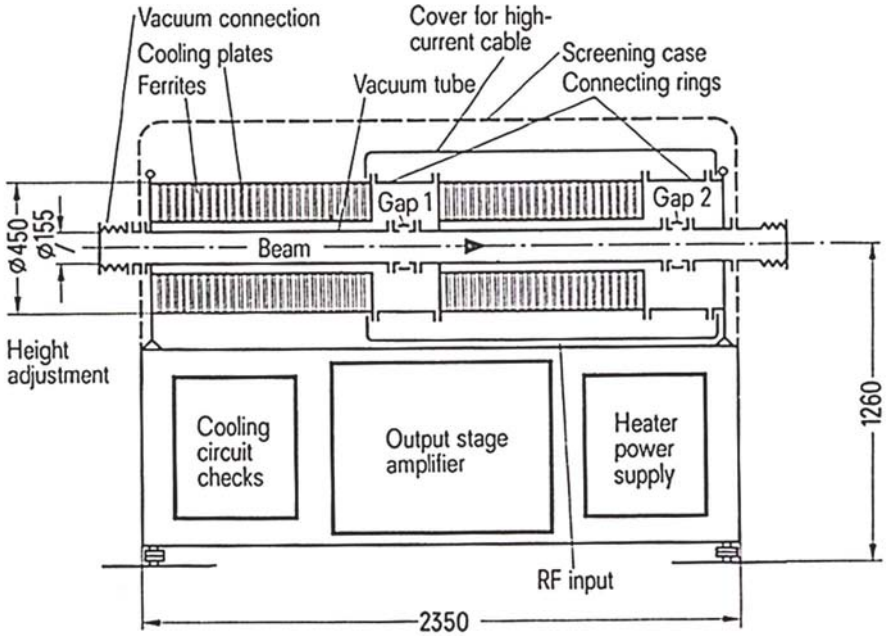

Fig. 3.10. Schematic drawing of one of the ferrite-loaded 3 to 10 MHz cavities; dimensions in mm.

The most complex task, the preparation of the beam for LHC, could only be mastered by adding a set of special RF systems operating at 20, 40 and 80 MHz to the main system [18]. From these systems the second example is chosen, a set of two special cavities operating at 80 MHz required for rapidly increasing the longitudinal focusing of the bunches destined to LHC just before extraction to the SPS [20]. These cavities produce a total of 600 kV and are pulsed for a brief moment prior to extraction. A damping antenna in the cavity suppresses higher-order electromagnetic modes which would adversely affect beam stability. TRIUMF contributed significantly to the design, construction and testing as an in-kind contribution of Canada to the LHC project. Figure 3.11 shows one of the cavities under test.

This battery of RF systems is used to produce a high-brightness proton beam for LHC [21]. The LHC requires short, intense bunches containing over 10^{11} protons of high transverse brightness, i.e. maximum transverse phase space density and a bunch to bunch separation of 25 ns or 50 ns. This beam is configured in the PS, the role of the SPS being restricted to acceleration from 25 GeV to 450 GeV, the LHC injection energy.

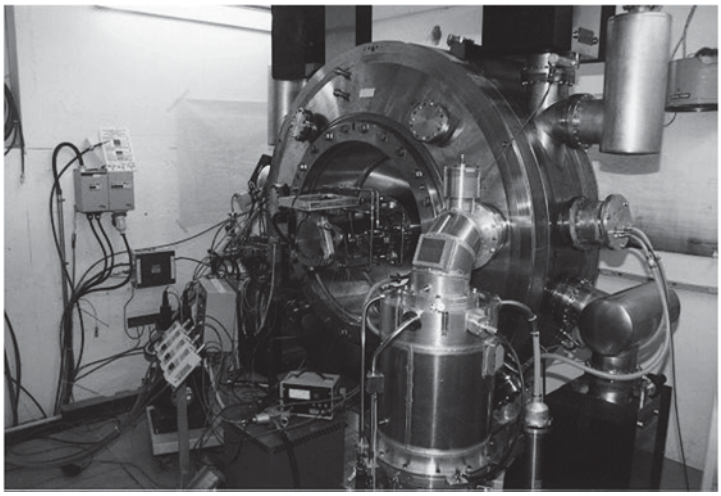

Fig. 3.11. Eighty-MHz RF cavity and 400 kW tetrode amplifier in the foreground in the test stand [20].

The main RF system cannot operate at 40 MHz corresponding to the 25 ns bunch separation. Hence, this bunch spacing is produced in steps during the acceleration cycle with the final steps just before extraction. Eight bunches are injected into the PS having six times the final intensity by using two cycles of the PSB producing each time one bunch in each of its four rings. After acceleration to 2.5 GeV, where the beam is less vulnerable to instabilities, the bunch train is compressed in time and two consecutive bunches are combined resulting in a bunch train of four bunches spaced by 300 ns, which is reduced to 100 ns in the subsequent triple splitting. All this is performed by the main RF system of three independent groups of three cavities each with the same voltage and phase. Figure 3.12 shows the beam during these manipulations, with the coloured lines marking the position of the bunches in time as a function of their relative position along the orbit. Using all cavities in all groups in unison, acceleration is pursued to 25 GeV where two consecutive bunch splittings take place resulting in the desired 25 ns spacing (for 50 ns only one splitting is performed). The first division of bunches is performed by the 20 MHz system, the second by the 40 MHz system while the main RF is off. In the final step of this virtuoso choreography, yielding 48 bunches of proper spacing, each bunch is longitudinally compressed to 4 ns by a rapid increase in the 40 MHz voltage and adding the full voltage of the 80 MHz system.

It is in this or similar schemes of bunch manipulation [18] that the PS RF systems display their full potential excelling in precise tuning, timing, phase and voltage control, testimony to their extraordinary flexibility and capacity, the result of continuous improvements over the years.

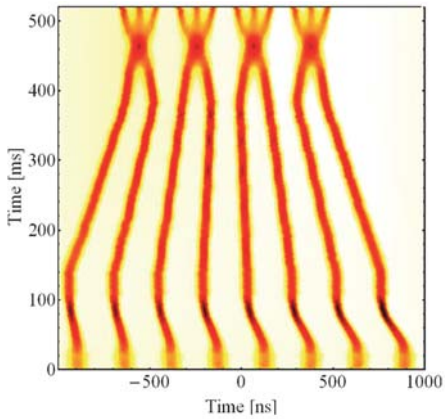

Fig. 3.12. Evolution of the bunch train between injection and at 2.5 GeV showing bunch train compression, combination of bunch pairs and triple splitting. Ordinate: time during the cycle; abscissa: longitudinal position of bunches along the orbit in terms of time [21].

3.4 Boosting PS Beam Intensity

Karlheinz Schindl

By the mid-1960s, CERN's 26 GeV Proton Synchrotron accelerated routinely ~ 10^{12} protons per pulse, a performance largely exceeding its design. However, at this level there were signs of saturation, in particular at injection energy (50 MeV) where a phenomenon called "space charge" appeared to limit the intensity. With new potential clients — the ISR and the SPS — on the horizon, a study on how to increase the output beam intensity of the PS to ~ 10^{13} protons per pulse (ppp) was launched. The space charge limit is brought about by the Coulomb force between the protons in a beam repelling each other and, therefore, working against the external focusing. The limit is strongly dependent on beam energy, and, during acceleration, the repulsive force gets weaker while the beam becomes stiffer. Hence, the limit is lowest at PS injection and it was overcome by raising the injection energy from 50 MeV to 800 MeV (kinetic) moving the limit up by a factor eight with an expected similar increase in intensity. A study of several alternatives led to the adoption of a very compact, slow-cycling 800 MeV synchrotron with four superimposed rings, the PS Booster (PSB) [22, 23], and re-use of the existing 50 MeV Linac. Operating each of the four rings (radius 25m, 1/4 of the PS) with five bunches at their individual space charge limit and transferring these four bunch trains sequentially to the PS would potentially deliver the desired 10^{13} protons to the PS.

The PSB was constructed between 1968 and 1972 after a very significant stumbling block was removed by diplomatic rather than technical skills: the PSB is the first accelerator ever built straddling an international border (Switzerland and France), paving the way for the much bigger accelerators also stretching across the border later. It was integrated in the PS injector chain in 1973, right away raising the PS output to 5×10^{12} ppp, just in time for the neutrino physics experiments with Gargamelle (Chapter 3.1).

It was the first particle accelerator with synchrotron rings stacked on top of each other. The four superimposed rings feature separate dipole (32) and quadrupole (48) magnets (as opposed to the PS where guide fields and gradients are generated by "combined-function" magnets) [24]. Each of them is a vertical stack of four magnets with a common yoke (Fig. 3.13). Their coils are connected in series and energized by one big power converter, while correction loops operating with rather small currents enable the guide and focusing fields to be adjusted for each ring. The stringent requirements on field quality and equality between rings gave rise to extensive studies of the prototype magnet stacks. The cross-section of both the magnet yokes and the coils were chosen large: the former mainly for better field quality, resulting in a relatively low magnetic field of ~ 0.6 T at 800 MeV, and the latter for minimizing integrated cost (construction + 10 years of operation). These latter features proved invaluable for later raising the PS Booster ejection energy to 1 GeV and 1.4 GeV. A further step to 2 GeV is planned.

A novel scheme [25] was also introduced to power the main magnets from a static power supply, rather than from a motor-generator set with a flywheel for energy storage, which draws constant active power from the mains as in the PS. Since the direct current varied between 200 and 3000 A during the acceleration cycle, this implied a power variation of about 7 MW. In order not to perturb the mains (voltage variation $< \pm 0.25\%$), the reactive power had to be compensated by a passive filter. A second passive filter was installed to ensure that the sinusoidal shape of the CERN mains voltage is maintained without parasitic oscillations at other points of the network (distortion < 0.5%). This system works satisfactorily for repetition times as low as 1.2 s, lower repetition times showed resonance effects in the generators of the main Geneva hydro-electric power plant (Verbois).

Twelve low-cost kicker magnets for injection and ejection of novel design with short rise or fall times were built using thyratrons instead of the unreliable pressurized spark gaps and introducing ferrite-loaded pulse steepening lines which, depending on the task of the kicker, shortened either the rise or fall time of the deflecting field to less than 50 ns [26]. The design had to be modified later to provide the longer beam pulses required by the new client, ISOLDE, and the higher voltage for the new top energy [27].

Fig. 3.13. One (out of 16) magnet periods showing the four superimposed rings. From right to left: dipole (green); vacuum chambers in straight section (grey); another dipole; a quadrupole triplet (focusing-defocusing-focusing, orange); dipole; RF equipment for beam acceleration (grey).

The path to design performance and beyond

The path to design performance proved arduous. Obstacles were addressed one by one, profiting from a few key developments in accelerator physics and technology.

- The focusing in the accelerator was programmed to quickly reduce, during acceleration, the adverse effects of space charge (unavoidable at injection).
- The five bunches conspired to oscillate in a coherent manner and these coupled bunch oscillations leading to beam loss presented a hard limit. The PS Booster was not the first accelerator to suffer from such instabilities, but it was the one where a deeper understanding of this phenomenon was developed leading to the first electronic feedback system effectively damping these oscillations [28].
- A new Linac 2, still 50 MeV, but with up to 150 mA beam current, was built, replacing in 1978 Linac 1 which proved unable to reach 100 mA as specified; two further measures limited the adverse effects of space charge: new multipole correctors intended to compensate magnetic imperfections and an additional RF system operating at the second harmonic of the main system lowered the peak line density of bunches.

These developments and inventions, together with many other improvements, allowed the PS Booster to reach its design intensity of 10^{13} ppp by 1974, 3×10^{13} by 1985, and eventually 4.2×10^{13} by 2003 (Fig. 3.14).

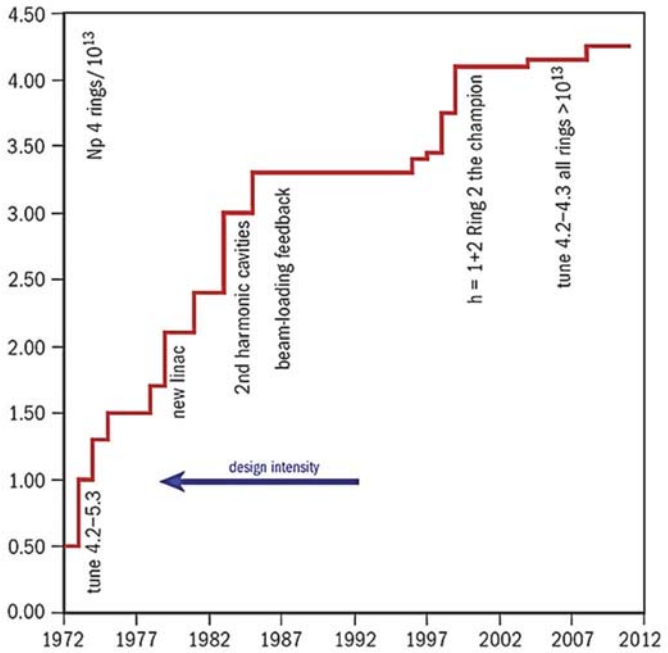

Fig. 3.14. The PSB peak intensity (sum of four rings) over the years. Major hardware additions and improvements are highlighted. (Adapted from [22].)

Also in the 1980s, the PSB got involved in ion acceleration, starting with deuterons and alphas, making its way through the Periodic Table to lead with the advent of Linac 3. This programme gave rise to numerous developments (RF, beam diagnostics) mainly to cope with ion intensities as low as 10^8 ions per pulse — five orders of magnitudes lower than proton beams within the same super-cycle. Since 1991 it replaced the aging CERN synchrocyclotron as proton source for ISOLDE.

In the LHC injector chain

In line with CERN's tradition of using existing accelerators as injectors for new machines, the LHC programme was no exception. It required a further increase of the top energy of PSB to 1.4 GeV and the replacement of the RF systems to deal with one instead of the originally used five bunches per ring [27]. In a further upgrade step the PSB ejection energy will be once more increased to 2 GeV and Linac 2 will be replaced by the new 160 MeV H^- Linac 4 as injector [29]. By this time, the PS Booster will be, in many parts, a new machine, while maintaining in the future its inherent versatility so successfully demonstrated in the past.

3.5 Capacitive Energy Storage Replaces Flywheel

Jean-Paul Burnet

The magnetic field in the 101 bending magnets of the proton synchrotron (PS) is cycled between 0.11 T at injection energy of the protons (1.4 GeV kinetic) to 1.25 T at top energy (26 GeV) with a repetition time of 2.4 s. About 6 to 8 million cycles are executed each year. The coils of this magnet string are in series representing an impedance of 0.32 Ω and 0.9 H and requiring a current of 5.5 kA at top energy. The active power for operating this string peaks at 40 MW at the end of the acceleration when the increase in stored magnetic energy reaches a maximum. After a constant period of about 0.2 to 0.3 s at top energy (flat top), the stored energy in the magnets has to be reabsorbed by the power supply, respectively by the energy storage system, during the ramp-down of the magnetic field implying a negative peak of 40 MW at the start of the ramp (Fig. 3.15). This power swing exceeds by far what could be tolerated by the mains in case of direct coupling though the average power is only 4 MW. The energy had therefore to be efficiently stored — a real engineering challenge. The original solution was energy storage in the rotational kinetic energy of the two rotors of a large motor-generator set acting as a flywheel. The set was supplied by industry and was replaced in 1968 in order to shorten the cycle time by a factor two to three. The new set shown in Fig. 3.16 consisted of a 6 MW alternating current (AC) motor and a 90 MW direct current (DC) generator providing a maximum of 6 kA at 12 kV [30].

The rotors had a total weight of 90 t capable of storing 233 MJ at 1000 rpm. The speed of the rotors decreased by 5% during ramp-up time while the motor absorbed 6 MW and, during ramp-down, the reflowing stored energy in the magnets peaking at 12 MJ reaccelerated the rotor to nominal speed.

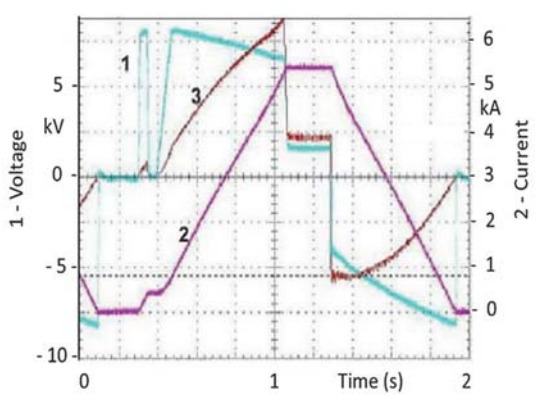

Fig. 3.15. The PS 26 GeV/c cycle: 1 voltage; 2 current; 3 active power 10 MW/div., vs. time [31].

Fig. 3.16. The 2nd generation PS main magnet power supply with the motor in the foreground.

Since maintenance of this set by industry came to an end and no supplier could be identified for a replacement, studies of alternative solutions were initiated in 2003. After discarding a solution with batteries due to their limited lifetime and energy storage in superconducting coils for lack of industrial products, the solution with storage in capacitors was preferred as they support nearly unlimited discharge cycles. Moreover, it could be constructed in a modular way based on industrial components. The new system, in operation since 2011, integrates two functions:

- Converting the AC current from the grid to DC current as required for the magnet powering;
- Storing the energy in six capacitor banks when not needed in the magnets [31, 32].

The capacitor banks are connected to the magnet string by six DC/DC converters which controls precisely current and voltage in the magnet circuit independently of the voltage of the capacitors. The voltage of the dry capacitors made from metalized self-healing Polypropylene decreases from 5 kV to 2kV during the ramping to top energy and increases again to 5 kV during ramp-down as shown in Fig. 3.17.

Only two AC/DC converters are connecting the system to the mains and supply the energy which is dissipated in the magnet coils. Since these losses peak at 10 MW during the flat top, the power rating of these converters is 5 MW. The DC/DC converters are based on medium-voltage power electronics produced by industry which allow a full control of the power flow in both directions depending on the requirement in the cycle. The key components are the 168 Injection Enhanced Gate Transistors (IEGT) which are used to switch currents up to 2.3 kA.

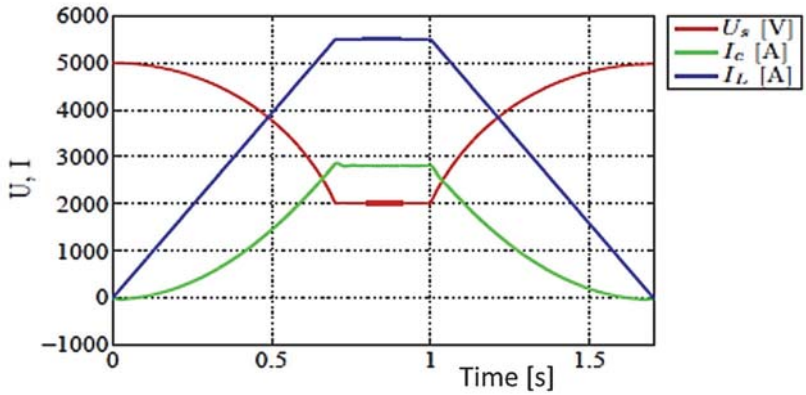

Fig. 3.17. Voltage (U_s) and current (I_c) of the capacitor bank with magnet current (I_l) as a function of time [32].

The system is complemented by output filters and a control system [33]. The total weight of capacitors is 60 t and they are placed inside six standard 40 foot shipping containers. Figure 3.18 gives an overall view of the new system. Although it was designed for high reliability, enough redundancy was included for functioning, albeit with reduced performance, in case of faults in one of the transformers, the AC/DC converter, the DC/DC converters, or in a capacitor bank. Its modular structure facilitates the management of spare components.

This novel CERN design has enabled the replacement of the aging large motor-generator set no longer supplied by industry with a fully solid-state system using the state of the art power electronics technologies. This system is a world first and, and being more efficient than the old motor-generator set, reduces the power demand from the mains to the strict minimum.

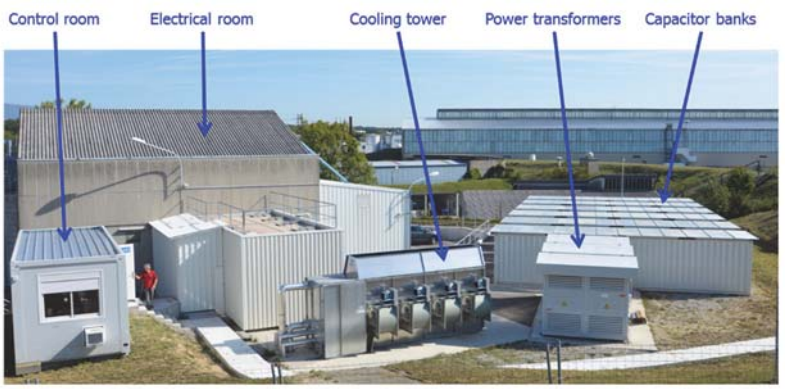

Fig. 3.18. The new power system for the PS main magnet.

3.6 Taking the Neutrinos by the Horns

Alan Ball

Four ingredients are needed to produce an intense muon neutrino (ν_μ) beam:

- An intense proton beam which is obtained by extracting all the circulating protons at top energy within one turn from the synchrotron [Highlight 3.2], the protons are focused onto a long thin target of low absorption materiel, often made from beryllium.
- A system to focus the secondary particles, produced in the target, charged pions (π) and kaons (K), which will eventually decay in flight into muons (μ) and muon neutrinos, the particles of interest. The challenge was to conceive a device that would focus a maximum of these "parent" particles, produced at different momenta and angles, towards the detector. The decay products, the neutrinos, are not focused by magnetic fields but are produced in roughly the same direction as the parent particles, ensuring maximum flux in the detector.
- A low density decay path, often in vacuum or helium gas, to ensure that parent particles do not interact with matter until they can decay in flight.
- An absorber to stop all hadrons remaining in the beam at the end of the decay path, so that only neutrinos and residual muons continue towards the detector.

The device invented by S. van der Meer [34] for the PS in the early 1960s was ingenious, revolutionary and decisive for obtaining neutrino beams of sufficient intensity. It is the *magnetic horn*. It works by focusing the secondary particles over a wide range of momenta and angles. The magnetic horn is a co-axial structure, typically 4–7 m long, where an electrical current flows along the inner conductor and returns along the outer conductor, producing a toroidal magnetic field in the space between them that is inversely proportional to the radius (Fig. 3.19). There is no field inside the inner or outside the outer conductors. By shaping the inner conductor, the integral magnetic field traversed by the particles can be designed to focus them towards the detector. The conductors are made as thin as possible to minimize absorption, yet sufficient to carry the large pulsed current.

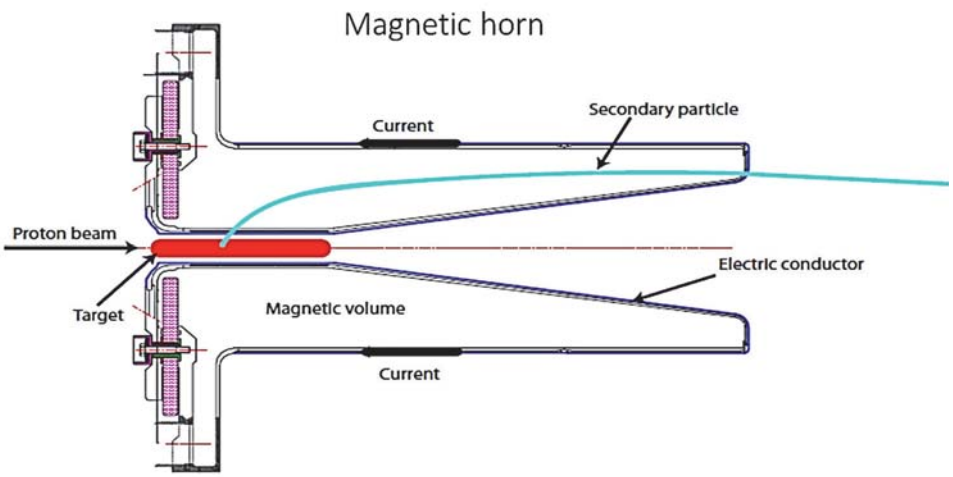

Fig. 3.19. Schematic cross-section of an early magnetic horn. The magnetic volume contains the azimuthal magnetic field.

Manufacturing the inner conductors of these co-axial lenses was no less of a challenge. The "neck" region of the horn was machined from a cylindrical bar of aluminium alloy, typically 70 cm long and 80 mm diameter. The machining could take nine months or more: the required "parabolic" form, of thickness of 1–5 mm, had to be cut and bored progressively with purpose-made tools, the swarf being removed at each stage to avoid piercing the thin-walled conductor. At larger diameters, the conductors were made from sheet metal rolled around a shaped mandrel and welded.

The insulated supports holding the inner conductor co-axially inside the outer conductor required precision adjustments. The inner conductor (Fig. 3.20) was cooled by water, sprayed from jets in the outer vessel and pulsed so there was no spray during the beam passage to add to the absorption. Insulation between conductors was complicated by power being supplied by capacitor discharge circuits giving a 200 μs pulse of up to 400 kA peak current at 12 kV. All this had to operate in an environment of high induced radioactivity.

The dimensions of this first dedicated neutrino facility at the PS [35] were quite modest; the decay tube was 15 m long and the detector, a heavy liquid bubble chamber (eventually Gargamelle) only a few metres downstream of the hadron stop. The total distance from target to detector was only 90 m.

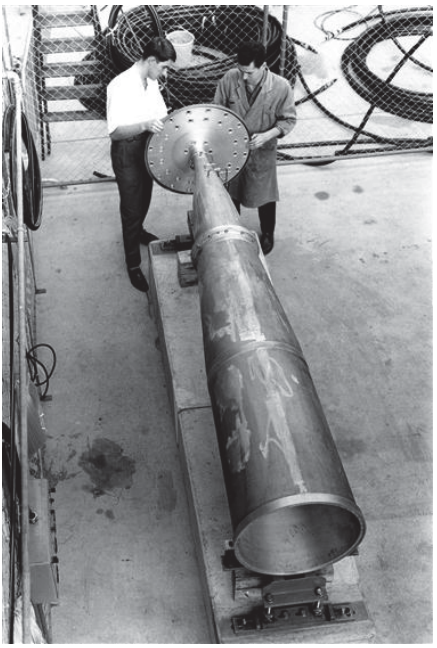

Fig. 3.20. Inner conductor of magnetic horn for neutrino beam.

Figure 3.21 shows the layout of the most recent accelerator-based neutrino source operated at CERN, the CERN Neutrino beam to Gran Sasso (CNGS) [36], located at 732 km downstream of CERN. The 400 GeV proton beam originated from the SPS (Chapter 5). The target is followed by the first magnetic horn; a second horn or "reflector" is used to improve the collection efficiency. The secondary particles travel in a kilometre-long evacuated decay tube to minimize losses from absorption and scattering. All remaining hadrons are stopped in a massive carbon and steel "filter". The muons emerging from the hadron stop were used to measure the divergence of the beam and to steer it so that it was centred on the detector.

Magnetic horns have been used in almost all wide-band neutrino beams so far constructed and planned in Europe, Japan and US. No other focusing device has provided the wide energy and angular acceptance, sign selection of secondaries and overall reliability.

Comparison of early PS beams with CNGS shows the impressive development of neutrino sources over a span of 40 years. This would not have been possible without magnetic horns, and the inventiveness and engineering flair of the teams that first constructed and operated them.

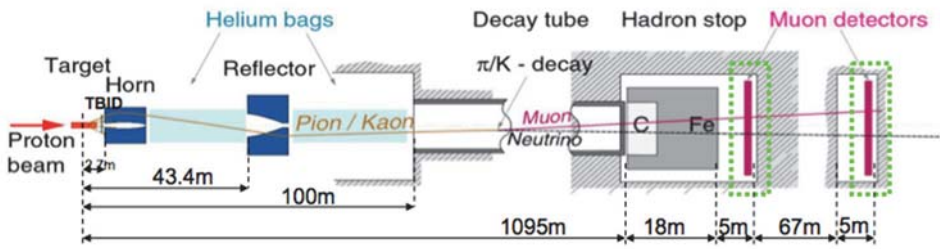

Fig. 3.21. Schematic layout of the neutrino source for CNGS [35].

3.7 OMEGA: Towards the Electronic Bubble Chamber

Werner Beusch and Emanuele Quercigh

Throughout the 1960s and 1970s bubble chambers were one of the principal instruments of particle physics research [Highlight 5.7]. These huge instruments were considered "facilities", which — similar to the accelerators providing the particle beams — were constructed and operated by teams of experts. These facilities provided the primary information allowing large collaborations to analyse a variety of new experimental data.

With increasing sophistication of the experiments, the use of electronic detectors, with the possibility of selecting particular phenomena and studying processes of small cross-sections, became obvious. The detector of choice was the spark chamber [Box 3.3], that could both visualise the events and be triggered to select a particular interaction. Placed in a magnetic field, the chambers provided position information of multiple particle tracks and hence their momenta. Spark chambers inside a magnet had been used at CERN since 1964. They provided data with statistics orders of magnitude larger than those of bubble chambers. The photographs of the sparks were measured with devices developed for bubble chambers. Later, these instruments, combined with novel algorithms for pattern recognition [37], provided particle trajectories without human intervention — major progress for analysis of large volumes of data.

With this background and as a part of the PS improvement programme a working group [38] was set up. The goal was to construct a large facility, the OMEGA spectrometer, also termed an "electronic bubble chamber", based on a strong magnet for good momentum resolution and large acceptance in order to investigate complicated interaction with many secondaries. A system of spark chambers with electronic readout and an efficient data handling was proposed.

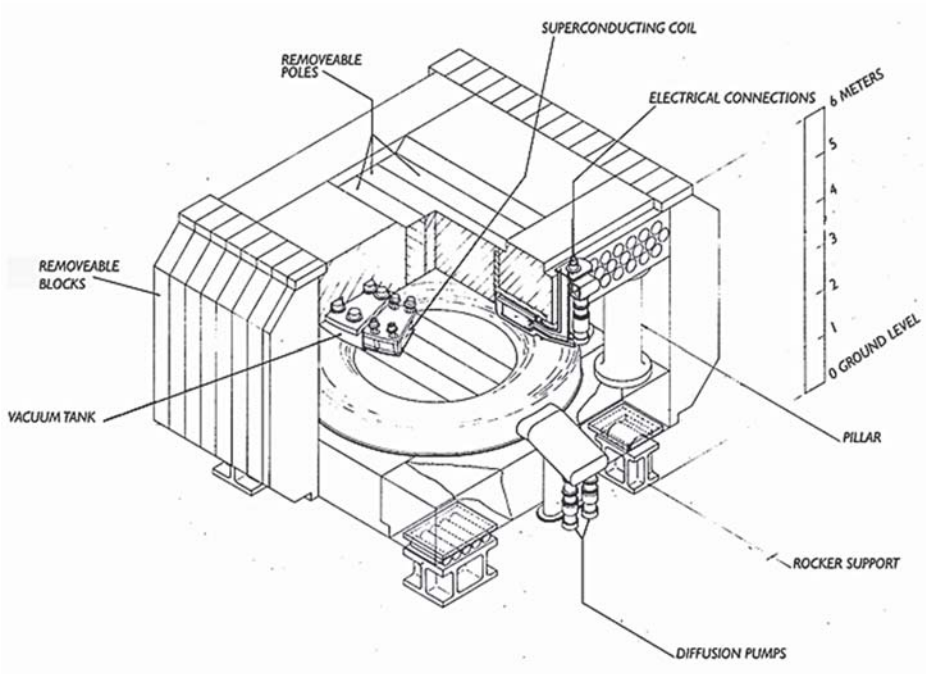

Fig. 3.22. Isometric view of the Omega magnet.

A courageous decision was taken: construct the largest superconducting magnet at the time (Fig. 3.22). The conductors were not to be the conventional ribbons in a bath of liquid helium, but tubes with the superconductor soldered to the surface, cooled by supercritical He at about 5 bar inside, a novel design that was intrinsically safe in case of a quench [Box 4.3]. The coils with an inner diameter of 3 m, producing a field of 1.8 Tesla, were clamped to the yoke. The supports had to withstand a force of about 2000 tons while transferring very little heat from the cold coils to the iron yoke. The whole system with helium compressors and liquefier was designed by a CERN team and realized by industry.

The readout of the spark chambers was another novelty. Tubes used in television cameras provided a stereo view of the chambers. The conversion of their video signal into coordinates useful for the physicists demanded some creative electronics design. Finding tracks from these data and reconstructing particle trajectories without human intervention was another new and difficult task.

Anticipating higher energy beams, increased precision of the momentum measurement was needed. As a first step two large (1.65 m × 3.2 m) drift chambers [Highlight 4.8] were constructed for a precise measurement of particles exiting the

magnet downstream. Furthermore, large counter hodoscopes for triggering, a Cherenkov counter for particle identification and an electromagnetic calorimeter completed the spectrometer.

This hybrid solution (spark and drift chambers) worked for a while with beams up to 200 GeV/c, but the need of a fully electronic system without the shortcomings of spark chambers and their readout was becoming urgent. In 1977 a proposal for improving the particle detector system (Omega Prime) was approved [39]. The choice of proportional wire chambers allowed higher beam flux, more refined trigger selection by allowing more time for a decision, better two-track resolution and easier data handling. The use of the proportional wire chambers was also essential for the flexibility required by the various experiments. More than 40,000 signal wires were mounted in the chambers, each wire precisely tensioned to 0.5 Newton. The readout of the signals had to be encoded on the chambers because the conventional use of a twisted pair cable for each chamber wire would have been impossible for this density of detectors. To provide time for a trigger decision a novel signal delay was developed. It was easily adjustable for the specific experimental conditions, could accept any number of hits, was storing the signals in electronic registers advancing in 20 ns steps and read out selectively the information pertaining to the triggered event. It was realized making very extensive use of electronic chips available at the time. The electronics, mounted on cards attached to the chamber frames, was designed and produced by members of the OMEGA group.

These experiments relied also on the variety and quality of the particle beams directed to OMEGA which at the beginning originated from the PS and later from the SPS. The SPS delivered initially 200 GeV/c protons and later up to 450 GeV/c protons, which required displacing the 1500 ton facility from its original position towards the centre of the West hall. Hyperon beams (baryons including at least one strange quark) and beams of sulphur and lead nuclei were delivered in addition to the more conventional beams. Omega received also a RF separated beam, i.e. a momentum selected hadron beam, with two RF cavities accepting or rejecting particles, depending of their time of flight between the cavities, hence on their mass.

With the increasing complexity of the experiments, the user groups, together with the OMEGA staff, developed the required detectors. Apparatus for better particle identification [40], for measurement of high energy photons, high resolution semiconductor detectors [Highlight 5.9] and new devices for triggering were devised.

The theory of strong interactions, QCD [Box 4.2], was tested with photons and hadrons. The study of hadron structure functions led to the very first published

SPS result. The study of high momentum transfer processes confirmed QCD. Experiments searching for glueballs, exotic particles made only of gluons and allowed by QCD, gave intriguing hints on their possible existence.

Motivated by the discoveries of charm and beauty [Box 6.4], OMEGA experiments contributed to the knowledge of the particles containing these quarks. The photon beam led to early observation of charm photo-production.

With the beam of lead nuclei hitting a target of lead, a series of experiments were performed with increasing sophistication, e.g. the use of an array of silicon pixel micro-detectors as main tracking devices to cope with the high multiplicity of tracks — a first for particle physics. It allowed the observation of particles containing up to three strange quarks. Their enhanced production rate, later confirmed by other experiments, was OMEGA's evidence for a new state of matter produced in lead-lead collisions at SPS energies.

This advanced, very flexible and steadily evolving facility operated from 1972 to 1996. It provided the basis for a wide range of experiments, overall 48. It relied not only on a number of leading-edge technologies but also on their successful integration and led to a number of important physics results. For a complete report on OMEGA physics published up to 1996 see [41].

3.8 ISOLDE: Targeting a New Era in Nuclear Physics

Helge Ravn

Since the early days of CERN research was carried out on properties of radioactive nuclei far from stability. Such nuclei play an important role in many areas of science ranging from fundamental nuclear interactions and astrophysics to material science and medical applications. These nuclei were created by irradiating targets with beams from the SC and later from the PS-BOOSTER. After irradiation the targets were transferred to the nuclear chemistry laboratory by the "Student-Running-As-Fast-As-Possible" (SRAFAP) method. There, aqueous phase chemical separation methods were applied to isolate the produced isotopes of interest. Scandinavian groups in particular were very active in studying and mapping the formation cross-sections of the new range of nuclei made available by the high energy protons reactions at CERN.

A very complex mixture of many isotopes of each element is produced in these reactions, next to impossible to study with the techniques available then. Only a breakthrough in new experimental techniques would solve this dilemma. It came about when the nuclear chemists realized that an accelerator technique — electromagnetic isotope separation — could be developed to achieve the desired

selection. The combination of this technique with chemistry provided high-purity samples of radioisotopes with a specific mass number *A* and atomic number *Z*.

One further obstacle had to be removed, requiring another invention and development. The inherent delay introduced by the "SRAFAP" off-line method limited the studies to nuclei with half-life > 10 minutes. This limitation was overcome by developing an on-line system, in which "chemically intelligent" targets were irradiated in an external proton beam. The chemical element of interest released selectively from the target was allowed to diffuse in a pipeline to the ion source of the mass separator from where mono-isotopic ion-beams emerged. To achieve this for all chemical elements a number of technological challenges had to be overcome, such as replacing the wet radiochemical techniques incompatible with the vacuum and high voltage requirements of an ion source.

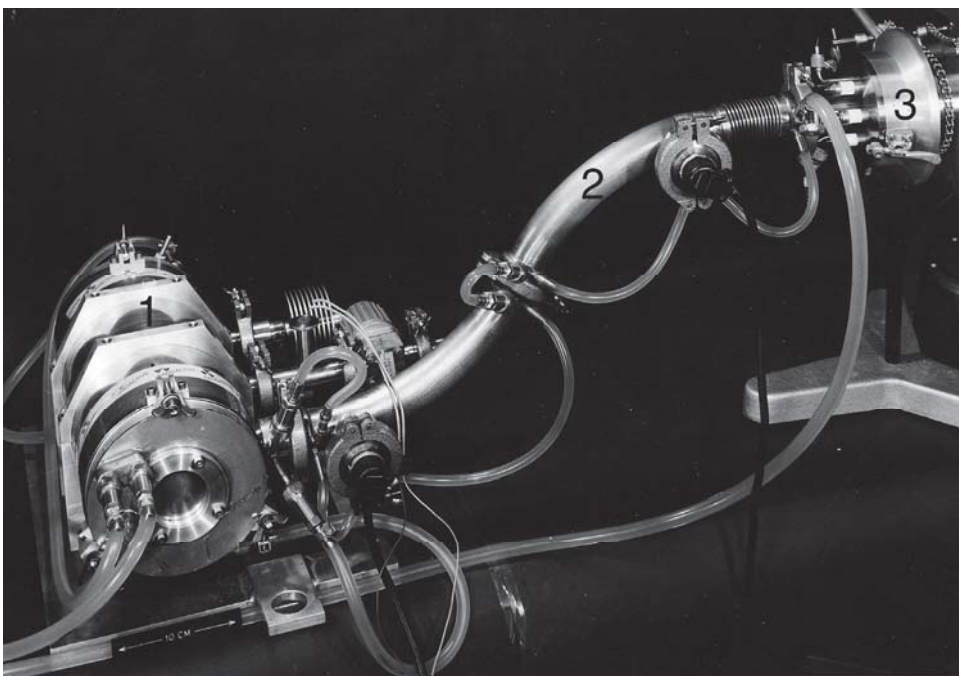

Fig. 3.23. The water cooled target vacuum-chamber (1) with its proton beam entrance window is pumped through the 1 m long vacuum tube (2) leading to the ion-source vacuum chamber (3). The target material (1) is molten lead or bismuth at 850 K. Inside (2) is the heated transfer line that allows the vapour of selectively released mercury isotopes to diffuse into the ion source.

Crucial for success was the understanding of the kinetics of this chemical mass-transport which allowed to separate the radioactive reaction products from the bulk target material and transferring them into the accelerator ion-source. This was solved by a vacuum-distillation process, often at temperatures above 2200 K. In the early system shown in (Fig. 3.23) the various steps in the process can be clearly identified [42]. It was thus that ISOLDE, the Isotope Separator On Line DEvice, was born. This system, invented at CERN by the ISOLDE group and the ISOLDE collaboration, allowed for the first time to continuously produce pure beams, e.g. of all the known mercury isotopes as well as discovering many new ones. Even the alchemist's dream of converting lead into gold was achieved by collecting the short-lived ^{197}Hg isotope from this first molten-metal accelerator-target and letting it decay into the stable gold isotope!

The speed of this separation process is governed by several factors: diffusion of the products out of the target material to its surface; desorption into the vacuum phase; adsorption and desorption steps encountered in collisions with the walls of the transfer-tube leading to the ion source and similar processes on the interior walls of the ion source. To assure the proper operation of the ion source, this process had to be performed in a vacuum of $< 10^{-4}$ Torr which also set the limit to the evaporation of the target matrix and other vapours accompanying the radioactive species at 10^{-8} mol/s [43]. For each element to be produced a separate unit had to be developed with its specific target and container material, temperature environment and ion-source type [44].

During the 50 years of CERN-ISOLDE and the ISOLDE collaboration target and ion-source units have been developed for about 60 of the chemical elements [45] providing more than 2000 individual ion-beams. For a typical example of one of these modern units see Fig. 3.24.

In addition to molten metal targets a number of high temperature — up to 2400 K — solid material targets were developed. With this method isotopes with half-lives as short as a few milliseconds could be studied.

In another development, high temperature chemical reactions inside the target were exploited for the first time to convert refractory elements into volatile chemical compounds, which then could be transported into the ion source. For example, the hafnium isotopes produced in a 2600 K tantalum-foil target can only be released from the Ta surface by letting them react with CF_4 gas continuously added to the target in order to form the volatile HfF_4.

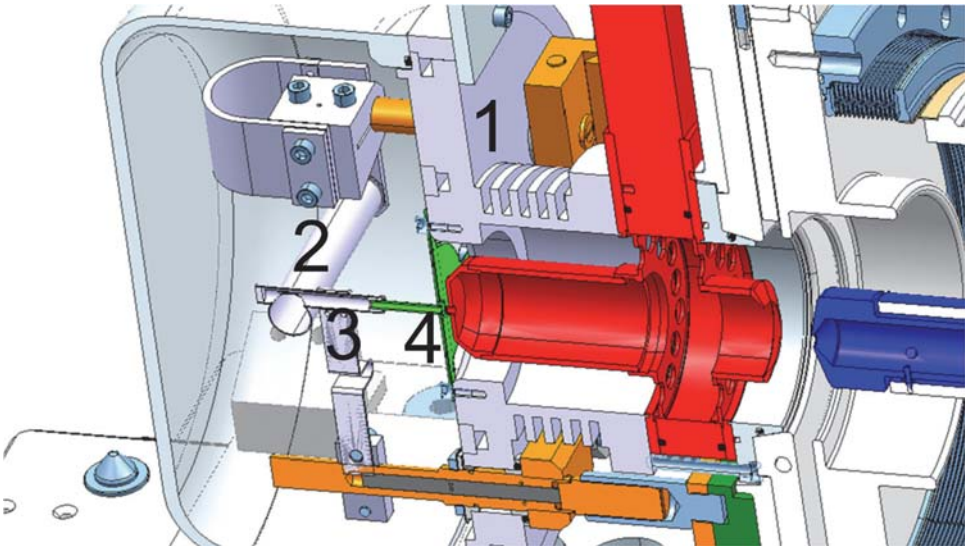

Fig. 3.24. Cut through the 30 by 30 cm universal vacuum chamber (1) containing the integral target, transfer-line and ion-source block which can be connected to the accelerator front end at 60 kV potential. In this example the 20 cm long Tantalum cylinder (2) contains a $^{235}UC_x$ target matrix kept at 2300 K. The released nuclei are conducted via a 5 cm long transfer line (3) to a 4 mm tubular ionizer (4) from which singly charged ions can be extracted into the accelerator to the right. By directing e.g. up to three laser beams opposite to the ion-beam direction a highly selective and efficient, stepwise resonant laser ionization is achieved. This target unit is equipped with a vacuum valve and quick connectors allowing rapid and remote exchange with an industrial robot.

Progress at ISOLDE in the beam production was paralleled by major progress in experimental methods developed to make best use of the radioactive ion-beams. Examples are the experiments based on methods adopted and adapted from atomic physics: optical pumping, laser spectroscopy atomic beam techniques, and mass spectrometry. Remarkably, due to a large degree of synergy between the accelerator and experiment communities, new accelerator techniques were developed based on some of these “imported” experimental methods.

A very successful invention of this type is the stepwise resonant laser ionization developed for many elements by CERN and the ISOLDE collaboration. While first used in the laser spectroscopy experiments in determining nuclear radii, it was adapted to become the primary ion-source as described in Fig. 3.24 [46].

It was the conjunction of these new technologies described that the vision of 1967 could finally be fulfilled [47]. The ISOLDE target and ion-source concept became the heart of today’s efficient radioactive ion accelerator REX ISOLDE [48].

3.9 The CERN n_TOF Facility: Catching Neutrons on the Fly

Enrico Chiaveri

High precision neutron cross-section data are of importance for a wide variety of research fields in basic and applied nuclear physics: In nuclear astrophysics data on neutron–nucleus reactions are essential to understand the production of heavy elements in the Universe, which occurs mainly through neutron capture processes during the various phases of stellar evolution. In nuclear technology, renewed interest in nuclear energy production has triggered studies aimed at developing future generation systems that would address safety, proliferation and waste concerns. For these applications the available nuclear data for many nuclides are of insufficient accuracy or even not existing.

Based on these motivations and given that the PS can produce proton pulses of very high intensity, the neutron Time-Of-Flight facility n_TOF has been proposed and constructed at CERN [49, 50], Fig. 3.25. It is based on the insight that such an intense proton bunch extracted from the PS could produce an intense pulse of spallation neutrons, produced in a wide range of energies and a correspondingly large spread in velocities. Thus, the neutron arrival time at a detector, located far downstream from the target, gives the neutron velocity and hence, its kinetic energy. Measuring precisely the neutron-time-of-flight produces a beam of neutrons with excellent energy resolution.

Commissioning and operation started in 2001 with performances ultimately matching design after a substantial optimization of shielding. The PS provides up to 8×10^{12} protons per pulse every 1.2 seconds (or multiples thereof). These proton pulses of 20 GeV/c momentum impinge on a 1.3 ton cylindrical lead target 40 cm in length and 60 cm in diameter producing a bunch of 2×10^{15} neutrons of 6 ns width. The high neutron flux, the low repetition rates and the excellent relative energy resolution, reaching values as low as 3×10^{-4} for 1 eV to 10 KeV neutrons, open new possibilities for high precision cross section measurements from thermal to a few GeV energy on stable and, importantly, radioactive isotopes.

The n_TOF target [51] is cooled by a 1 cm water layer and with a subsequent layer of 4 cm of water or borated water (H_2O + 1.28%H_3BO_3, fraction in mass). Initially fast neutrons are moderated into the desired energy spectrum, which ranges down to thermal energies. The experimental area (EAR1) begins at 182 m from the spallation target and has a length of 7.9 m. Along the evacuated beam line a sweeping magnet (200 cm long, 44 cm gap and 3.6 Tm bending power) deflects and removes the charged particles in the beam. In a typical experiment, a sample is placed in the neutron beam, and the reaction products are detected with

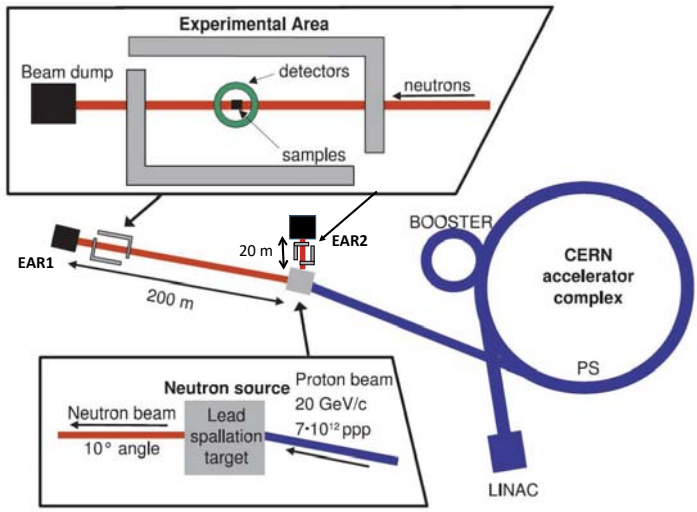

Fig. 3.25. Layout of the n_TOF facility [51].

specialized instruments. The reaction probability is measured as a function of the incident neutron flight time and hence its energy.

To extend the measurements on stable and short-lived isotopes, with very low cross sections or available only in extremely small quantities, the n_TOF Collaboration proposed the construction of a new experimental area (EAR2) at a shorter distance from the spallation target to exploit a much higher neutron flux [52]. It was convenient and advantageous to build the new experimental area on the surface, directly above the pit hosting the spallation target, which is located approximately 20 m below the surface. This layout reduces the time-of-flight between target and detectors by a factor 10 and increases the neutron flux by a factor of around 25 relative to EAR1. It allows measurements of correspondingly smaller samples, of smaller cross sections or in a shorter time. The factor 10 shorter flight time is also a crucial advantage for the study of radioactive substances. The spread in arrival time ΔT of neutrons in an energy interval ΔE and hence the necessary sensitive time of the detectors is reduced by the same factor 10. Reducing the measurement time reduces the dominant background from the decay of the radioactive isotope under study. The total gain in sensitivity of up to a factor of 250 relative to EAR1 means that isotopes with half-lives as short as a few months can now be studied [53].

The CERN n_TOF facility is worldwide unique due to its very wide energy spectrum and intensity of neutrons. It is home of a rich and in many ways unique scientific programme [52].

References

1. E.D. Courant, M.S. Livingston and H.S. Snyder, The strong-focusing synchrotron—a new high energy accelerator, *Phys. Rev.* **88**, 1190 (1952).
2. E. Regenstreif (ed.), *The CERN Proton Synchrotron*, *Vol. 1*, CERN-1959-029 (CERN, Geneva, 1959). http://dx.doi.org/10.5170/CERN-1959-029.
3. E. Regenstreif (ed.), *The CERN Proton Synchrotron*, *Vol. 2*, CERN-1960-026 (CERN, Geneva, 1960). http://dx.doi.org/10.5170/CERN-1960-026.
4. E. Regenstreif (ed.), *The CERN Proton Synchrotron*, *Vol. 3*, CERN-1962-003 (CERN, Geneva, 1962). http://dx.doi.org/10.5170/CERN-1962-003.
5. S. Gilardoni and D. Manglunki (eds.), *Fifty Years of the CERN Proton Synchrotron*, *Vol. I*, CERN-2011-004 (CERN, Geneva, 2011). http://dx.doi.org/10.5170/CERN-2011-005.
6. S. Gilardoni and D. Manglunki (eds.), *Fifty Years of the CERN Proton Synchrotron*, *Vol. II*, CERN-2013-005 (CERN, Geneva, 2013). http://dx.doi.org/10.5170/CERN-2013-005.
7. L. van Hove, M. Jacob, Highlights of 25 years of physics at CERN, *Phys. Rep.* **62**, 1 (1980).
8. S. Weinberg, Unified theory of elementary-particle interactions, *Sci. American*, July 1974.
9. P. Musset and J.P. Vialle, Neutrino physics with Gargamelle, *Phys. Rep.* **39**, 1 (1978).
10. R.K. Bock, Data processing for bubble chambers, *Nucl. Phys*. **36B**, 229 (1994).
11. M. Gell-Mann, *Phys.Lett*. **8**, 214 (1964) and
    G. Zweig, An SU(3) Model for Strong Interaction Symmetry and its Breaking,
    CERN preprints 8182/Th-401, and 8419/Th-412. http://cds.cern.ch/record/570209?ln=en.
12. R.P. Schutt (ed.), *Bubble and Spark Chambers* (Academic Press, New York, 1967);
    G. MacLeod and B. Maglic (ed.), *Informal Meeting on Film-less Spark-Chamber Techniques and Associated Computer Use*, CERN-1964-030 (CERN, Geneva, 1964).
    http://dx.doi.org/10.5170/CERN-1964-030.
13. M. Giovanozzi and C Steinbach, p. 91 in *Fifty Years of the CERN Proton Synchrotron*, *Vol. I*, S. Gilardoni and D. Manglunki (eds.), CERN-2011-004 (CERN, Geneva, 2011).
    http://dx.doi.org/10.5170/CERN-2011-004.91.
14. D. Fiander, Hardware for a full aperture kicker system for the CPS, *Proc.1971 Particle Accelerator Conference*, Chicago, USA (1971) 1022.
15. J. J. Bleeker, C. Germain, M. Thivent and R. Tinguely, Development of an electrostatic septum for the slow ejection of the CPS, *Proc. 8th Intern. Conf. on High Energy Accel*., Switzerland, Geneva (1971) 113.
16. J. Borbugh, M. Hourican and M. Thivent, Consolidation Project of the electro-static Septa in the CERN PS Ring, *Proc. IEEE Particle Accel. Conf.,* USA, Chicago IL (2001) 1541.
17. C. Bertone *et al.*, Studies and implementation of the PS dummy septum to mitigate irradiation of magnetic septum in straight section 16, *Report CERN-ACC-2014-0043* (2014); http://cds.cern.ch/record/1697680?ln=en.
18. R. Garoby, RF gymnastics, pp. 69-89 in *Fifty Years of the CERN Proton Synchrotron*, *Vol. I*, S. Gilardoni and D. Manglunki (eds.), CERN-2011-004 (CERN, Geneva, 2011).
    http://dx.doi.org/10.5170/CERN-2011-004.69.
19. H.C. Grassmann, R. Jankovsky and W. Pirkl, New RF System for the 28 GeV Proton Synchrotron at CERN, *Siemens Review,* **XLIV** (4), 164-170 (1977).
20. D.G. Grier, E. Jensen, R. Losito, A.K. Mitra, The PS 80 MHz cavities, *Proc.6th Europ. Part. Acc. Conf. (EPAC'98),* Stockholm, Sweden (1998) pp. 1773-1775.

21. H. Damerau, A. Findlay, S. Gilardoni and S. Hancock, RF manipulations for higher brightness LHC-type beams. *Proc. Int. Part. Accel. Conf. (IPAC'13)*, Shanghai, China (2013) 2600-2602.
22. K. Hanke, M. Chanel and K. Schindl, The Booster hits 40, *CERN Courier* July/August 2012.
23. M. Chanel, The Proton Synchrotron Booster (PSB), in *Fifty Years of the CERN Proton Synchrotron*, *Vol. II*, S. Gilardoni and D. Manglunki (eds.), CERN-2013-005 (CERN, Geneva, 2013). http://dx.doi.org/ 10.5170/CERN-2013-005.
24. A.M. Ašner, G. Brianti, M. Giesch and K.D. Lohmann, The PS Booster Main Bending Magnets and Quadrupole Lenses, *Proc.3rd Int. Conf. on Magnet Technology,* Hamburg, Germany (1970) 418.
25. H. Fiebiger, Y. George, B. Godenzi, G. Legras and F.V. Völker, Thyristor static compensator for the CERN intermediate booster accelerator, *ACEC Rev.* **3**, 2 (1980).
26. A. Brückner, Kicking Protons, Fast and Cheap, *Proc. 4th IEEE Part. Accel. Conf.*, Chicago, USA (1971) 976.
27. M. Benedikt, P. Collier, V. Mertens, J. Poole, K. Schindl (eds.), *LHC Design Report*, *Vol. 3: the LHC Injector Chain*, edited CERN-2004-003 (CERN, Geneva, 2004). http://dx.doi.org/10.5170/CERN-2004-003-V-3.
28. F. Pedersen and F. Sacherer, Theory and performance of the longitudinal active damping system of the CERN PS Booster, *Proc.6th IEEE Part. Accel. Conf.,* Washington DC, USA, (1975) 1398.
29. K. Hanke *et al*., Status of the Upgrade of the CERN PS Booster, *Proc.4th Int. Part. Accel. Conf.*, Shanghai, China (2013) 3939.
30. O. Bayard (ed.), *La Nouvelle Alimentation de l'Aimant du Synchrotron à Protons du CERN*, *Vol. 1: Description Générale*, CERN-1971-010 (CERN, Geneva, 1971). http://dx.doi.org/10.5170/CERN-1971-010.
31. C. Fahrni, A. Rufer, F. Bordry and JP. Burnet, A multilevel power converter with integrated storage for particle accelerators, in *Proc. Power Conversion Conference (PCC '07)*, Nagoya, Japan (2007) 1480.
32. C. Fahrni, Principe d'alimentation par convertisseurs multiniveaux à stockage intégré – Application aux accélérateurs de particules, CERN-Thesis-2008-154 (2008); http://cds.cern.ch/record/1375850?ln=en.
33. F. Boattini, JP. Burnet, G. Skawinski, POPS: The 60MW power converter for the PS accelerator: Control strategy and performances, *Proc.European Conference on Power Electronics and Applications, (EPE 2015),* Geneva, Switzerland (2015), *Report CERN-ACC-2015-0098* (2015); http://cds.cern.ch/record/2056733?ln=en.
34. S. van der Meer (ed.), *A Directive Device for Charged Particles and its Use in an Enhanced Neutrino Beam*, CERN-1961-007 (CERN, Geneva, 1961). http://dx.doi.org/10.5170/CERN-1961-007.
35. M. Giersch *et al*., Status of magnetic horn and neutrino beam, *Nucl. Instr. & Meth.* **20**, 58- 65 (1963).
36. K. Elsener, E. Gschwendtner and M. Meddahi, Right on target: CNGS gets off an excellent start, CERN Courier, November 2006, http://cerncourier.com/cws/article/cern/29753.
37. P.M. Blackall, G.R. MacLeod and P. Zanella, The analysis of spark chamber pictures using a raster scan technique, *IEEE Trans. Nucl. Sci.* **NS13**, 34 (1966).
38. W.F. Baker, The OMEGA project: Proposal for a large magnet and spark chamber system, NP Internal Report 68-11 (1968); https://cds.**cern**.ch/record/299898.

39. W. Beusch, OMEGA PRIME: a project of improving the omega particle spectrometer, CERN/SPSC/77-70 (1977); cds.**cern**.ch/record/345021?ln=en.
40. R.J. Apsimon *et al*., A ring imaging Cherenkov detector for the CERN Omega spectrometer – the design and recent performance, *Nucl. Instr. & Meth. A* **248**, 76-85 (1986).
41. M. Jacob and E. Quercigh (eds.), *Symposium on the CERN OMEGA Spectrometer*, CERN-1997-002 (CERN, Geneva, 1997). http://dx.doi.org/10.5170/CERN-1997-002.
42. A. Kjelberg and G. Rudstam (eds.), *The ISOLDE Isotope Separator Facility at CERN*, CERN-1970-003 (CERN, Geneva, 1970). http://dx.doi.org/10.5170/CERN-1970-003.
43. H.L. Ravn, Experiments with intense secondary beams of radioactive ions, *Phys. Rep*. **54**, 201 (1979).
44. H.L. Ravn and B. Allardyce, On-line mass spectrometers, p. 363 in *Treatise on Heavy-Ion Science* **8**, ed. D. Allan Bromley (Plenum Press, New York, 1989).
45. The ISOLDE Radioactive Ion Beam Facility; http://isolde.web.cern.ch.
46. V.I. Mishin *et al*., A chemically selective laser ion source for on-line mass separation, *Nucl. Instr. & Meth. B* **73**, 550 (1993).
47. J. Bondorf, A short summary of the concluding discussion, p. 681 in *Proc. Int. Symposium on Why and How Should We Investigate Nuclides Far Off the Stability Line, Lysekil,* (1966), eds. W. Forsling, C.J. Herrlander and H. Ryde, *Ark. Fys.* **36** (1967).
48. REX ISOLDE, http://rex-isolde.web.cern.ch/
49. http://public.web.cern.ch/public/en/research/n_TOF-en.html.
50. C. Rubbia *et al*., A high resolution spallation driven facility at the CERN-PS to measure neutron cross sections in the interval from 1 eV to 250 MeV, CERN/LHC/98-002-EET (1998); http://cds.cern.ch/record/357112/files/lhc-98-002.pdf.
51. C. Guerrero *et al*., Performance of the neutron time-of-flight facility n TOF at CERN, *Eur. Phys. J. A* **49**, 27 (2013).
52. C. Weiss, E. Chiaveri, S. Girod, V. Vlachoudis and the n_TOF Collaboration, The new vertical neutron beam line at the CERN n_TOF Facility - design and outlook on the performance, *Nucl. Instr. & Meth. A* **799**, 90-98 (2015).
53. E. Chiaveri *et al*., Proposal for n TOF Experimental Area 2 (EAR-2), CERN-INTC-2012-029, INTC-O-015 (2012); http://cds.cern.ch/record/1411635.